ACTIVE PROKARYOTIC COMMUNITIES ALONG A THERMALLY AND GEOCHEMICALLY VARIABLE TRANSECT IN GUAYMAS BASIN HYDROTHERMAL SEDIMENTS

Zena Cardman

A thesis submitted to the faculty at the University of North Carolina at Chapel Hill in partial fulfillment of the requirements for the degree of Master of Science in the Department of Marine Sciences.

Chapel Hill
2014

Approved by:

Andreas Teske

Carol Arnosti

Barbara MacGregor

ABSTRACT

Zena Cardman: Active prokaryotic communities along a thermally and geochemically variable
transect in Guaymas Basin hydrothermal sediments
(Under the direction of Andreas Teske)

The microbial inhabitants of deep-sea vents are genetically and metabolically diverse,

and often make a living at the edge of biological temperature limits. Guaymas Basin, a nascent

spreading center in the Gulf of California, provides a unique environment in which to study

prokaryotic communities across a range of thermal and geochemical niches. Unlike most vents,

Guaymas is blanketed in thick sediments, ranging from 3ºC to 200+ºC within half a meter below

the sea floor. Microbial mats, including one nicknamed "Megamat," serve as bull's-eyes for

subsurface hydrothermal activity. Here we explore Megamat's subsurface, spanning low-

temperature (3º), low-methane (0.3mM) to high-temperature (85º), high-methane (3+ mM)

sediments, and the 16S rRNA-based phylogeny of active prokaryotes therein. Pyrosequencing

revealed the fewest OTUs yet highest Shannon-Wiener diversity within the hottest sediments.

Sequences of *Sulfurimonas* were nearly ubiquitous, and sequences from the heterotrophic MBGB

dominated outside the mat's perimeter. Putative methane cyclers were most abundant within the

methane-saturated mat center, including ANME-2c, *Methermicoccaceae*, Guaymas-specific

ANME-1 groups, and a deeply-branching, novel group, "Guaymas Methanomicrobia." The

expected *Deltaproteobacterial* sulfate reducers were not common in this survey; in fact

Archaeoglobus and *Thermodesulfobacteria* sequences were recovered in exponentially higher

abundance in the hottest sediments. Major groups were most similar outside of Megamat and at

its edge, in contrast with strikingly core-specific communities in central mat samples. The mat's

edge appears to be a transition zone hosting sequences found both in the central mat and in bare

sediment, while the distinct community assemblages within central Megamat highlight

horizontal and vertical variability in Guaymas Basin. Together, these data provide insights into

community changes with temperature and substrates at high resolution over small spatial scales.

For Emil Davis

ACKNOWLEDGEMENTS

TABLE OF CONTENTS

LIST OF FIGURES

LIST OF TABLES

LIST OF SYMBOLS AND ABBREVIATIONS

μM   Micromolar

ANME   Anaerobic Methanotroph, an uncultured group

AOM   Anaerobic Oxidation of Methane

CH_4 Methane

cmbsf   Centimeters Below Sea Floor, with the sediment-water interface at 0 cmbsf

CO_2 Carbon Dioxide

$\delta^{13}C$ Delta ^{13}C, a measure of the ratio of stable Carbon isotopes in parts per thousand

DIC   Dissolved Inorganic Carbon

H_2S Hydrogen Sulfide

mM   Millimolar

OTU   Operational Taxonomic Unit, defined in this manuscript at 97% similarity

PCR   Polymerase Chain Reaction

RNA   Ribonucleic Acid

rRNA   Ribosomal Ribonucleic Acid

SO_4 Sulfate

ACTIVE PROKARYOTIC COMMUNITIES ALONG A THERMALLY AND GEOCHEMICALLY VARIABLE TRANSECT IN GUAYMAS BASIN HYDROTHERMAL SEDIMENTS

1. INTRODUCTION

Guaymas Basin, a nascent spreading center in the Gulf of California, offers a unique environment in which to study microbial communities across a broad range of thermal and geochemical niches. Unlike most vent sites, Guaymas is blanketed in a hundreds-of-meters-thick layer of organic-rich sediments of pelagic and terrigenous origin (Calvert 1966, Von Damm et al. 1985). Hydrothermally active spots pepper the basin where magmatic sills intrude and discharge fluid through tectonic fractures (Einsele et al. 1980, Lonsdale and Becker 1985). The hydrothermal fluids are alkaline, and reach temperatures up to 315ºC. As it advects upward, the high-temperature vent fluid interacts with and alters the sediments, facilitating metal sulfide precipitation, pyrolysis of hydrocarbons and organics, and other diagenetic processes (Kawka and Simoneit 1987). Compared to bare lava vents, the metal content of Guaymas fluids is a few orders of magnitude lower (Von Damm et al. 1985, Von Damm 1990).

Methane concentrations in Guaymas fluids reach 12-16mM, two orders of magnitude higher than bare lava vents, and with higher concentrations and lighter carbon isotopic composition compared to mantle outgassing. The $\delta^{13}C$-CH_4 here ranges from –50 to –43‰, implicating a thermocatalytic origin (Welhan 1988). *Archaeal* methanogenesis is a second source of methane at some locations, often indicated by lighter $\delta^{13}C$ CH_4 signatures. Methane sinks include the anaerobic oxidation of methane across a wide range of in situ temperatures

(Biddle et al. 2011, Holler et al. 2011), as well as simply the release of methane into the overlying water column.

These hydrothermal fluids are rich in pyrolysis products and biogenic substrates: the aforementioned methane, as well as other light hydrocarbons, short-chain organic acids, and ammonia (Martens 1990). Guaymas fluids thus carry to the shallow sediments a smorgasbord typically only available in the deep subsurface. A robust community of methanogens, methane oxidizers, sulfate reducers, and other microorganisms make a living here (Dhillon et al. 2003, Teske et al. 2002); these groups range from psychro- and mesophilic to high-temperature-tolerant and even hyperthermophilic. They enrich the hydrothermal fluids in sulfide and CO_2, to in turn be utilized by their upstairs neighbors: sulfur-oxidizing *Beggiatoa* mats, which serve as surficial bulls-eyes for localized subsurface hotspots (Jannasch et al. 1989, Gunderson et al. 1992).

Bare sediment away from these colorful mats is the temperature of Guaymas bottom water throughout (3-4ºC), and shows little or no signature of hydrothermal fluid. Beneath the mats, temperatures typically exceed the known thermal limits of life within the upper half-meter of sediment. The physicochemical environment can vary wildly over even a centimeter scale, both laterally and vertically (McKay et al. 2012). Temperatures and hydrothermal flux can also vary temporally (H. Mendlovitz and B. White, personal communication). Horizontal advection of fluid (suggested in Kawka and Simoneit 1987, Lonsdale and Becker 1985) may result in lower temperature discharge in the mud surrounding mounds. This horizontal transport may significantly confound our interpretation of geochemical profiles.

Biogeochemical, lipid biomarker and sequence-based evidence for complex microbial communities has been detected in these sediments (Teske et al. 2002; Dhillon et al. 2003, 2005),

yet a great deal of work remains before we understand exactly who is active, how they affect and are affected by geochemical microniches, or how much biogeochemical variability exists. Studies of subsurface microbial diversity across multi-dimensional gradients are especially lacking. Here we look in detail at one mat-covered seep site through a transect of sediment cores, coordinating prokaryotic community structure with physicochemical niches over small scales. This RNA-based study gains insight into the active community present in surface and subsurface sediments, including some of the highest-temperature sediments from which RNA has been recovered to date.

2.   METHODS

2.1   Site description

At the time of sampling, Megamat was a broad, mostly white *Beggiatoa* mat (Figure 1), spanning about 5-10 m diameter at 2,002 m water depth and approximately 27ºN 00.445, 111ºW 24.530. Fluids were hot and rich in hydrothermal petroleum degradation products such as LMW organic acids, alkanes, and methane; hydrocarbons could often be seen bubbling up from the mud. While we cannot know the exact history of any one site, we do know that visible mats can grow or shrink over the course of one year, or possibly during even less time. A currently cold site could have a relatively recent hot history, or vice versa. A large microbial mat could change size or disappear with changes in subsurface hydrothermal flow. Extensive push coreing may further affect a mat. Nevertheless, Megamat as it existed in 2008 is described above and was the source of samples for this study.

The samples were taken along a five-point transect: (1) from the center of the mat, (2) a hot site within the mat's perimeter, (3) a less-hot site at the mat's edge, (4) another cooler site just outside the mat's perimeter, and (5) a cold site from bare sediment several dozen meters

away. From each of these transect points was collected: (i) sediment for microbial community analysis, (ii) sediment for geochemical profiling, and (iii) temperature profiles in the upper 40cm of subsurface. Figure 2 shows a cartoon of this transect in relation to Megamat; these samples are summarized in Table 1.

2.2   *Sample collection*

The deep submersible *HOV Alvin* was used to collect temperature profiles and coordinating push cores during dives 4485, 4486, and 4491 in December 2008. Temperature was measured *in situ* with *Alvin*'s external heat flow probe (shown in Figure 1c), at 5 or 10cm depth intervals over the upper 40 or 42cm of sediment. Freshly recovered push cores (3 inches diameter and on average 17cm length) were sectioned shipboard on the *R/V Atlantis* at 2cm intervals, immediately frozen in liquid nitrogen, and stored at -80°C until processing. Sediments from 0-2cmbsf and 6-8cmbsf were used for geochemical and microbiological analysis.

Temperature probes, microbiology sediment cores, and geochemistry sediment cores were taken as closely as possible for coordinating samples along the transect. For sites (2), (3), and (4), microbial data and geochemical data are from cores effectively touching each other, i.e. <1cm from edge to edge, or 3cm from center to center, and temperature profiles were measured directly adjacent to their respective cores. For site (1), sediment cores and coordinating temperature profile were a few cm apart. At site (5), the geochemical and microbiological cores were approximately 6cm apart, and the temperature profile an additional few cm away. It should, however, be noted that several temperature profiles were taken within a 1m radius of site (5) and all revealed 3°C over the entire upper 40cm of sediment.

Throughout this manuscript, these five sites will often be referred to by microbiology core number only, representing microbial community, geochemistry, and temperature data in:

"bare sediments" (4485-5), "edge of Megamat" sediments (4486-19, 4486-24), and "central Megamat" sediments (4486-13, 4491-7). The bare sediment site at 4485-5 serves as a sort of "background" sample, but only in the sense that this sediment is far removed from Megamat. It is still within the general area of many scattered Guaymas hotspots, and its biogeochemistry is likely still influenced by proximity to hydrothermal flow in spite of its cold, unchanging 3ºC temperature profile and relatively low, unchanging, unsaturated methane concentrations over at least the upper 20cmbsf.

2.3   *Geochemical porewater analysis*

Sulfate and sulfide concentrations were measured from porewater, separated from 15mL sediment by centrifugation; the resulting supernatant was 0.2um filtered. One 1mL subsample was acidified with 50uL 50% HCl and bubbled with nitrogen for 4 minutes to remove sulfide before shipboard sulfate measurement on a 2010i Dionex Ion Chromatograph (as previously described in Martens et al. 1999). For sulfide, a second 1mL porewater subsample was preserved with 0.1mL 0.1M zinc acetate, until measured spectrophotometrically (Cline 1969). For methane analysis, sediment was sealed in serum vials with 0.1M NaOH. Headspace methane concentrations were obtained using gas chromatography with flame ionization detection. Stable carbon isotopes of methane and DIC were measured from porewater, separated from approximately 50mL of sediment by centrifugation and 0.2 μm filtration, and quantified by gas chromatography and isotope ratio mass spectrometry on a Hewlett Packard 5890 GC with Finnegan Mat 252 IRMS.

2.4   *RNA extraction and amplification*

Selected frozen sediment core subsections (0-2cmbsf and 6-8cmbsf, 30-40g wet weight each) were thawed by vortexing with trichloroacetic acid lysis buffer (McIlroy et al. 2008). To

lyse cells, samples were agitated 2x45 seconds in an MSK-Zellhomogenisator (B. Braun Biotech

International, Melsungen, Germany) with sterile 0.1 and 0.45μm diameter glass beads. Nucleic

acids were precipitated overnight at –20ºC, in 0.6 volume isopropanol (MacGregor et al. 1997).

The precipitate was pelleted by 30 minutes' centrifugation at 2800rpm in an Eppendorf 5702/R

with A-4-38 swinging-bucket rotor, and resuspended in nuclease-free water. RNA was purified

via multiple pH 5.1 phenol, phenol-chloroform, chloroform-isoamyl alcohol separations

(following Stahl et al. 1988, MacGregor et al. 1997). Following another overnight precipitation

at –20ºC (in 0.7 volume isopropanol and 0.5 volume ammonium acetate), RNA was pelleted

(again by a 30 minute centrifugation), resuspended in nuclease-free water, further purified with a

Qiagen RNeasy RNA Cleanup Kit, eluted in 50μl nuclease-free water, and stored short-term at –

20ºC. Low concentrations of extracted total RNA (often ≤2ng/μl) necessitated amplification

prior to 454 pyrosequencing. SuperScript III One-Step RT-PCR with Platinum Taq DNA

Polymerase reagents (Thermo Fisher Scientific, Waltham MA) were used according to the

manufacturer's instructions to reverse-transcribe rRNA to cDNA, then amplify the V5-V8 region

of 16S rRNA using universal primers 787F (5'-ATTAGATACCCNGGTAG-3', Roesch et al.

2007, Jorgensen et al. 2012) and 1391R (5'-ACGGGCGGTGWGTRC-3', Lane et al. 1985,

Jorgensen et al. 2012). This primer combination gives 98% coverage of *Bacteria* and *Archaea*

with one mismatch (Jorgensen et al. 2012). As a control, parallel PCR reactions for each sample

were performed without reverse transcriptase; absence of a product in this case ruled out DNA

contamination, thus indicating amplification only of cDNA derived from RNA. Amplified

concentrations of this 600bp product after 30 cycles in a Bio-Rad iCycler Thermal Cycler, and

the final volume sent for sequencing, are shown in Table 2.

2.5   *454-pyrosequencing and phylogenetic analysis*

The V5-V8 product was barcoded and pyrosequenced at the UNC Chapel Hill Microbiome Core Facility using Roche 454 technology. Returned sequences were denoised and filtered for read quality with Qiime (Caporaso et al. 2010), and multiplexed reads were assigned to samples. De novo operational taxonomic units (OTUs) were picked at 97% sequence similarity, and representatives were chosen for each OTU. These representatives were checked for chimeras using Qiime's ChimeraSlayer, then assigned domain- and phylum-level taxonomy with the SILVA aligner and SSU reference database (arb-silva.de/aligner) (Pruesse et al. 2007). Finer-resolution classification was achieved through alignment with Arb software (Ludwig et al. 2004). Final phylogenetic trees were constructed with the neighbor-joining distance method with Jukes-Cantor correction (Saitou and Nei 1987); bootstrap confidence values were assigned from 1,000 tree iterations (Felsenstein 1985).

2.6   *Clone library synthesis from extracted DNA and RNA*

As comparison for our 454 pyrosequencing dataset – and to ground-truth those shorter reads within phylogenetic trees – clone libraries were constructed with near-full-length *Archaeal* 16S sequences from cores 4491-7 (central Megamat) and 4486-24 (edge of Megamat). Total genomic DNA was extracted from approximately 0.5g sediment and RNA from 2.0g sediment with MoBio PowerSoil DNA and RNA kits. A Bio101 Thermo Savant FP120 fast prep bead beater was used to lyse the cells, but kit protocols were followed thereafter. Near full-length 16S rRNA genes were amplified with *Archaeal* primers A8f and A1492r (Teske et al. 2002) in a Bio-Rad iCycler Thermal Cycler. PCR reactions were carried out as previously for Guaymas Basin 16S samples (Biddle et al. 2012). Euryarchaeotal-specific primers A8f and Eury498r (Burggraff et al. 1994) were also used. Reverse transcription was carried out with a Takara OneStep RT-

PCR kit and the same primer combination as above, A8f and A1492r, also as described in Biddle et al. 2012. As with the 454 pyrosequencing data presented here, neighbor-joining phylogenetic trees were constructed with Jukes-Cantor correction (Saitou and Nei 1987) and bootstraps were assigned after 1,000 tree iterations (Felsenstein 1985).

3.   RESULTS AND DISCUSSION

3.1   Temperature and geochemical gradients throughout Megamat

In the bare sediment several dozen meters away from the edge of Megamat (4485-5), temperatures are a constant 3.0ºC (Guaymas Basin bottom water temperature) over at least the upper 40cmbsf. Just outside the mat's perimeter, temperatures reach 10-11ºC by 2cmbsf, and increase almost linearly over 40cm depth to 84 or 101ºC (4486-19 and 4486-24, respectively). Within Megamat-covered sediments, core 4486-13 is already 26ºC at the surface, 85ºC by 6cmbsf, and 163ºC at 40cmbsf. Core 4491-7, a few meters further into Megamat from the 4486 transect, reaches 112ºC at depth. These temperature measurements of course represent only one point in time within a highly variable environment, and are not from the exact location of either their corresponding microbiology or geochemistry cores. The data nevertheless give valuable and concrete context for the localized conditions in Megamat prior to sampling, and provide an approximation for temperatures experienced by these sediments.

Surface sediment temperatures reveal the patchy and often hot conditions experienced by the *Bacterial* mat community. Subsurface temperatures, meanwhile, grant insight into hydrothermal flow below. The 11 temperature profiles shown here in Figure 3, and the three-dimensional temperature field presented by McKay et al. 2012, show a wide range of thermal environments in Megamat's subsurface. Mat perimeter profiles are typically less than 15ºC from 0-2cmbsf, and increase linearly to 100ºC by 40cmbsf. Within the central mat subsurface,

sediments experience much steeper thermal gradients: often hotter than 30° or even 50°C by 2cmbsf, exceeding 100°C by 20cmbsf, and leveling off above 150°C from 20-40cmbsf. Some Megamat sediments reach 200°C by 30cmbsf (McKay et al. 2012). Metabolic and thermal zonation appears to be more compressed in the upper subsurface within central mat sediments than at the mat's edge, and much more so than in bare sediments.

Sulfate in Guaymas Basin penetrates the sediment at or near seawater concentrations, approximately 28mM. While geochemistry core 4486-14 is unfortunately lacking a data point at 0-2cm depth, we can assume sulfate enters this core at a similar concentration. At the edge of Megamat there is little vertical decrease of sulfate, changing only 2-5mM throughout the core. In central Megamat, sulfate is sharply "consumed" over the upper few centimeters: down to 2mM by 6-8cmbsf in core 4486-14 and below detection limits by 8-10cmbsf in core 4491-12 – keeping in mind, of course, that with variable horizontal and vertical flow it is difficult to infer microbial activity from geochemical profiles alone. Low sulfate concentrations here, for example, could also be accounted for by sulfate-free or sulfate-depleted hydrothermal fluid permeating the sediments from below, rather than consumption by microbial metabolism.

Sulfide concentrations are low in surface sediments of all measured cores; 4491-12 within central Megamat is the only core with elevated sulfide concentrations (2.5mM) at the surface. Four of these five cores show a local sulfide peak at 10-14cmbsf, which, in tandem with decreasing sulfate profiles, suggests an active community of sulfate reducers at these depth horizons. Core 4486-14 is an exception, with low sulfide concentrations throughout, though notably this core experiences the highest temperatures over the upper 30cm, and is already above 100°C by 10cmbsf.

In our Megamat samples, methane concentrations are high in the subsurface: 1-2mM at 40cmbsf in all mat-associated cores, which is likely an underestimate due to outgassing during and after sample recovery. In central Megamat, porewater methane permeates the entire sediment column at near constant high concentrations. Upward movement of subsurface fluids may be significant enough to inhibit the isotopic expression of microbial methane cycling, and the nearly homogeneous $\delta^{13}C$ CH_4 signature seen in these cores appears to be influenced by subsurface abiogenic sources. Methane formed biogenically in sediments typically falls within the range of –42‰ to –105‰. This wide range depends heavily on active community composition and function, as well as temperature (Whiticar 1999). Abiotic methane, by contrast, is more typically within the range of –20‰ to –50‰; Guaymas porewater methane typically falls within this latter range, implying a predominantly thermocatalytic origin (Welhan 1988, Pearson et al. 2005).

While temperature may limit microbial activity in some of Megamat's hot, central sediments, core 4491-12 is a relatively cool 6°C at the surface, and does show some small amount of putative methane consumption in the upper 4cm of sediment. Porewater methane concentration at the surface of this core decreases while $\delta^{13}C$ methane is slightly enriched. Just inside the edge of Megamat, core 4486-24 reveals a broad sulfate-methane transition zone, with depletion of methane concentrations to near-zero from 10cmbsf upward, $\delta^{13}C$ from Guaymas hydrothermal fluid signature around –40‰ (Peter and Shanks 1992, Welhan 1988) at depth to nearly –25‰ at the surface, and a slight consumption of sulfate over the upper 8cm. Just outside the mat's edge methane is also apparently consumed, but less sharply than in 4486-24 and without the diagnostic $\delta^{13}C$ signature of methane oxidation. Far outside Megamat, in 4485-1, methane concentrations are lower (0.45mM at 15cmbsf) than in mat-associated cores at depth,

with barely a change in concentration throughout the core. There is a spike in the $\delta^{13}C$ of methane around 8cmbsf, nearly 10‰ heavier than the upper 6cmbsf, perhaps linked to the isotopically lighter DIC there.

The isotopic signature of DIC in that distant, bare-sediment core (4485-1) is markedly low between 5 and 13cmbsf, possibly implicating microbial remineralization of organic matter at these depths, though porewater concentration data is lacking for this core. In the peripheral sediments of Megamat, DIC concentrations are 10-15mM at 16cmbsf, and decrease down to 5mM at the surface; in hotter sediments, concentrations are not depleted in surface sections relative to concentrations at depth. Little change in $\delta^{13}C$-DIC is evident throughout any mat-associated cores, excepting a lighter signature in the upper 4cmbsf of 4491-12. In diffusion-dominated marine sediments, this would suggest microbial remineralization of organic matter.

In Guaymas sediments, geochemical profiles are complicated by advection, so the isotopic signatures may be artifacts of fluid transported horizontally from elsewhere. Rapidly-flowing hydrothermal fluids may also overwhelm any signs of authigenic microbial activity. Alternately, the relatively heavy $\delta^{13}C$-DIC may reflect limited microbial remineralization of organic matter in these cores, or a combination of Guaymas hydrothermal DIC near -9‰ and Guaymas bottom seawater near -0.6‰ (Pearson et al. 2005). In other words, this isotopic signature may be consistent with some mixture of HCO_3^--derived DIC and CO_2-derived DIC, or, depending on the pH, may be mostly CO_2 with little influence from organic matter remineralization.

Together, these data (summarized in Figure 4) show the clear influence of hydrothermal input within Megamat sediments compared to bare sediment. The profiles presented here also

illustrate the physicochemical patchiness of Guaymas Basin with steep gradients in electron donor and carbon availability between cores that were taken mere centimeters apart.

3.2   OTU abundance and Shannon diversity

Ribosomal RNA-based microbial community analysis comes with a caveat: cellular ribosome concentrations may differ between taxonomic groups or even individuals, so a greater presence of any particular lineage's 16S rRNA does not necessarily equate to cell abundance (Campbell and Kirchman 2013). That said, RNA degrades rapidly extracellularly, so it is expected to derive primarily from living cells. DNA, by contrast, may persist for longer periods in the sediment, and can be recovered from spores or dead cells, or as extracellular detrital DNA (Dell'Anno and Danovaro 2005). Obtaining a snapshot of actively transcribing prokaryotes is especially interesting in a hydrothermal environment like Guaymas Basin, where cells face biophysical stress at extreme temperatures.

Pyrosequencing yields were >1500 reads per core at each depth, and just shy of 30,000 reads total. Primers targeted both *Archaea* and *Bacteria* at the V5-V8 region. *Archaeal* sequences were the overwhelming majority in these samples, outnumbering *Bacteria* at least 2:1 in all cores, more than 5:1 in several cores, and more than 100x in core 4486-19 at 6-8cm depth. This was not the case for multiple other Guaymas Basin samples, extracted with identical methods, amplified with the same PCR master mix, and sequenced simultaneously on the same plate (L. McKay, personal communication), so primer biases are not implicated. Total *Bacterial* and *Archaeal* sequence reads per sample are summarized in Table 3. Operational taxonomic units (OTUs), picked in Qiime with a 97% similarity cutoff, are shown in Figure 5, and vs. sediment temperature in Figure 6.

In surface sediments (0-2cmbsf), OTU abundance is highest just outside the mat's edge. This edge-of-mat area may be a species-rich ecotone: a transition zone where both out-of-mat and inside-mat OTUs coexist. Excluding the bare sediment a few dozen meters away from Megamat (comparable in OTU abundance to 4486-24 and 4486-13), OTUs generally decrease from outside the mat to inside (Figure 5), but do not show a clear trend with subsurface temperature (Figure 6). At depth, however, OTU abundance is highest outside the edge of Megamat, and lowest in central sediments (Figure 5), and appears to decrease linearly with temperature (R > 0.6, Figure 6). This may indicate the stronger influence of temperature on OTU abundance at depth in the mat subsurface, versus perhaps a stronger influence of factors like substrate availability at the sediment-water interface.

The Shannon-Wiener index, (Shannon and Weaver 1963, Wiener 1948), also called Shannon Entropy, is frequently used in ecological studies to analyze species diversity and abundance, defined as:

$$H' = - \sum p_i \ln p_i$$

where p_i is the proportional abundance of individuals of species i. This value thus indicates both richness and evenness, accounting for rare species and weighting them relative to common species. Shannon diversity approaches zero as one group increases in relative abundance, and equals zero if only one group is present. With uncultured environmental samples, the microbial ecologist can substitute OTUs for species in this equation. H' is a useful and meaningful measure for comparing prokaryotic communities in soil and marine sediments (e.g. Hill et al. 2002, Heijs et al. 2007, Auguet et al. 2010). Shannon-Wiener diversity of course does not offer any information regarding diversity above the OTU level. For example, OTUs present here may

be all within a narrow phylogenetic range, or they may be widely spread across any number of

taxonomic groups. With this in mind, a more detailed look at 16S rRNA-based phylogenetic

classification will be discussed in section 3.3 of this manuscript.

Total prokaryotic community diversity is shown in Figure 7. At the sediment-water

interface in Megamat, H' is greatest in 4486-13, which experiences the highest temperatures of

these surface samples. Diversity is lowest elsewhere within Megamat's perimeter (4491-7), and

just outside the mat's edge (4486-24). The greatest diversity in 0-2cmbsf samples was found

farther outside the edge of Megamat (4486-19) and in bare sediments well beyond Megamat

(4485-5). At deeper depths, H' is highest within the cooler central-mat sediments (4491-7, vs.

hot central-mat 4486-13) and in bare sediment distant from Megamat (4485-5). It is lowest

outside of Megamat's edge (4486-19) and increases from just outside (4486-24) to just inside

(4486-13) the mat's perimeter.

Separating by domain-level classification, *Archaeal* H' (Figure 8a) is highest in surficial

sediments of 4486-13, the highest-temperature core within Megamat's perimeter. *Bacterial*

diversity (Figure 8b) is highest in the three surface samples outside of Megamat, and consistently

higher than *Archaeal* H' in each sample, excepting 4486-13 (both at the surface and 6-8cmbsf).

The highest-temperature sample in this study (4486-13 at 6-8cmbsf) hosted a low diversity of

both *Archaea* and *Bacteria* (Figure 9), though both were higher than H' for the other central mat

core, 4491-7, at 0-2cmbsf. No apparent trend existed for *Bacterial* diversity with temperature in

0-2cmbsf sediments, all of which were < 60ºC. *Archaeal* diversity, however, increased with

temperature in 0-2cmbsf sediments ($R^2 = 0.8$ including all samples, or $R^2 = 0.6$ for Megamat-

only sediments, excluding the bare sediment sample 4485-5 several dozen meters away). Deeper

in the subsurface, at 6-8cmbsf, *Archaeal* H' revealed a very weakly negative trend with

14

temperature ($R^2 = 0.4$). *Bacterial* diversity in sediments 6-8cmbsf showed the most striking

trend, decreasing linearly with temperature (0.9). *Bacterial* communities in these sediments may

be more sensitive to temperatures greater than 60°C, though diversity across all prokaryotes here

is likely affected by some combination of temperature and substrate availability, not to mention

grazing, interaction with viruses, competition, or other environmental factors. In any case,

temperature is clearly not the only influence on diversity, and the actual 16S rRNA-derived

community composition, discussed in the following section, paints a more nuanced picture of

active prokaryotes in these sediments.

3.3   *Prokaryotic community structure: 454 pyrosequencing*

Archaeal community composition (Figure 10a), both at 0-2cmbsf and 6-8cmbsf, appears

similar at the mat's edge (4486-22 and 4486-19) and well outside the mat (4485-5). Within

central Megamat, the two cores (4486-13 and 4491-7) are strikingly different in surface and

subsurface sediments. This emphasizes the horizontal and vertical variability even within the

perimeter of one Guaymas Basin microbial mat.

Marine Benthic Group B (MBGB, Vetriani et al. 1999) dominates *Archaeal* communities

outside Megamat and at the mat's edge, both in surface sediments and at 6-8cmbsf (Figure 10a).

This deeply-branching, heterotrophic group often dominates *Archaeal* 16S rRNA gene and 16S

rRNA transcript libraries, and is metabolically active in deep marine subsurface sediments

(Teske and Sørensen 2008, Biddle et al. 2006). Carbon isotopic signatures in *Archaeal*

phospholipids and cell biomass implicate this group as organic carbon assimilators (Biddle et al.

2006). While MBGB are often found with methane-rich sediments (Inagaki et al. 2006, Biddle et

al. 2006, Sørensen and Teske 2006), their abundance has also been linked to organic carbon and

ferric iron oxide, suggesting an iron-reducing, organic matter-degrading metabolism (Jorgensen

et al. 2012). Prevalence of MBGB in warm sediments here is consistent with previous studies of Guaymas Basin (Biddle et al. 2012).

In surficial bare sediments (4485-5) and the edge of Megamat (4486-19 and -24), *Methanosarcinaceae*, ANME-2c, GoM Arc I, Marine Benthic Group D (MBGD), MCG-15, and DHVE-6 are also found in moderate abundance. MBGD is commonly found in marine sediments (Teske and Sørensen 2008), including hydrothermal sediments (Takai and Horikoshi 1999). At depth, MBGD shares the sediment with MBGB as we approach the mat, though the latter decreases while MBGD increases. ANME-2c rRNA was also found in core 4486-24, just outside the perimeter of Megamat, where methane concentration profiles and $\delta^{13}C$ signatures indicate sulfate-dependent methane oxidation at this depth. ANME-2c sequences have often been associated with cold sediments replete in electron acceptor (Knittel et al. 2005), while ANME-1 (whose sequences were not frequently recovered in this 454 pyrosequencing survey) seems to tolerate sulfate limitation and turns up in fully-reduced environments (Lloyd et al. 2011, Knittel et al. 2005).

The two cores 4486-13 and 4491-7 taken from sediments in central Megamat are distinct from the other cores, and from each other. While both cores share high methane concentrations throughout the sediment column and contain sulfate only in their surficial layers, sulfide concentrations are significantly higher in 4491-7, and in-situ temperatures are significantly higher in 4486-13. At 0-2cmbsf: the active microbial communities of core 4486-13 are more diverse than those of 4491-7 and yield relatively evenly-distributed reverse-transcribed 16S rRNA sequences of *Archaeoglobus*, DHVE-6, DSEG-3, deeply-branching "Guaymas Methanomicrobia" (named for the first time in this text), and a few transcripts related to *Methermicoccaceae* and uncultured *Thermoplasmatales*. Core 4491-7, by contrast, is almost

entirely dominated by ANME-2c sequences in surface sediments (approximately 6°C *in situ*, vs.

the 26° surface sediments of 4486-13), though *Methanosaeta* and *Microarchea* (ARMAN-2,

Baker et al. 2006) sequences make cameo appearances. At depth in the hottest sediments, core

4486-13 sediments yielded approximately equal numbers of uncultured DSEG-3 and

Archaeoglobaceae sequences. Arb-based neighbor-joining phylogeny places these sequences

with the known *Archaeal* sulfate reducers of the genus *Archaeoglobus* (Klenk et al. 1997)

(Figure 12), as opposed to their non-sulfate-reducing sister taxa *Geoglobus* or *Ferroglobus*

within the *Archaeoglobales* (Tor et al. 2001). Core 4491-7 is more diverse at depth, including

members of *Methanomicrobiaceae*, methane-oxidizing ANME-2c, the thermoacidophilic genus

Aciduliprofundum, MBGD (and other uncultured Thermoplasmatales), and MCG.

Although *Bacteria* are overall less abundantly detected in each sample, they reflect

Archaeal population trends: similar major *Bacterial* groups dominating outside of Megamat and

at its edge, in contrast with distinctly core-specific populations in each of the central mat cores

(Figure 10b). Interestingly, core 4486-24 diversity very much resembles the 16S community

fingerprint of hot core 4491-7 at 6-8cmbsf, while in surface sediments this core is more similar

to those outside of the mat's surface area. Apparently, subsurface hot spot communities can

extend beyond the surface margins of a mat area, as previously observed at a mat area in the Gulf

of Mexico (Lloyd et al. 2010).

The nitrate-reducing, sulfur- and hydrogen-oxidizing genus *Sulfurimonas* (within the

Epsilonproteobacteria, Figure 11) is nearly ubiquitous (Campbell et al. 2006). Sequences from

this genus are abundant in surface sediments of core 4485-5 and at the mat's edge, and count for

95% of all *Bacterial* sequences found in core 4491-7 (the cooler of two central-mat cores).

Dehalococcoides-related sequences increase with proximity to the mat's edge in warm and cool

cores; *Psychromonas*, SAR202, and uncultured *Gammaproteobacteria* are also found at 0-2cmbsf in these cores. Core 4486-13 is again distinct: *Bacterial* populations here are split between *Thermodesulfobacteria*, *Marinitoga*, *Thermosipho*, and *Thermotoga*.

The sulfur-oxidizing *Beggiatoa* who so conspicuously drape the surface of these sediments are nowhere to be found at the molecular level (in this study, as in Kysela et al. 2005); even targeted sequencing surveys of *Beggiatoa* mats recover few of their phylotypes (Mills et al. 2004). While individual *Beggiatoa* cells are quite large in size, their intracellular volume is mostly filled by a gigantic vacuole, leaving little room for cytoplasm (Jannasch et al. 1989, Nelson et al. 1989). These giant filaments apparently do not possess any more copies of 16S rRNA transcripts in their limited periplasmic space than smaller mat affiliates.

At depth, *Sulfurimonas* sequences are common at the mat's edge (core 4486-24) in nearly equal abundance to JS1 sequences, and in the relatively cool central-Megamat sediments of 4491-7, from which candidate phylum OP9 sequences were also recovered. Outside the mat in subsurface samples, SAR 202 sequences dominate, with some contribution from the hydrogen-oxidizing, dehalogenating, anaerobic group *Dehalococcoides*. In core 4486-19, just outside the mat, WS1 sequences are also prevalent. Once again 4486-13 is markedly different, hosting *Thermodesulfobacteria* and unclassified *Firmicutes* transcripts at 6-8cmbsf.

Looking in greater detail at the presumed sulfate-reducing community reveals a conspicuous contrast in core 4486-13 versus other sediments (Figures 12 and 13). *Deltaproteobacteria* are common sulfate reducers in subsurface sediments, and include the typical partners in consortia with ANME *Archaea*, related to *Desulfosarcina* or *Desulfococcus* (Orphan et al. 2002, Knittel et al. 2003, Schreiber et al. 2010). *Deltaproteobacterial* sequences, however, are found only in very low abundance throughout any of these samples (Figures 11 and

12). In the hottest sediments (4486-13), sequences amplified from *Archaeoglobus* RNA dominate, orders of magnitude more abundant than *Deltaproteobacteria* sequences recovered from other samples, and about twice as abundant as the thermophilic, sulfate-reducing family *Thermodesulfobacteriaceae* found in 4486-13 sediments, by measures of percentage or even absolute RNA sequence recovery. *Archaeoglobus* and *Thermodesulfobacteriaceae* (found here in 4486-13 but nearly absent in other sediments) are known to be thermophilic, while the *Deltaproteobacteria* recovered in this survey (in low sequence abundance in nearly every sample but 4486-13) are not. The difference between sulfate-reducing communities in 4486-13 and elsewhere in Megamat may be due to extreme physicochemical fluctuations, or longer-term trends experienced by some portions of the mat. Temperature and hydrothermal flux in Guaymas Basin are highly variable not only spatially but also temporally, even over daily scales (H. Mendlovitz, personal communication).

Putatively methane-processing *Archaea* appear in divergent sequence abundances across all samples (Figures 14 and 15). Generally speaking, more of these sequences were recovered (as a percentage of total prokaryotes) from sediment inside and close to Megamat's perimeter than in bare sediments – consistent with the high concentrations of methane throughout these cores, versus bare sediments with relatively low porewater methane concentration. Outside the mat, the methane-cycling-related sequences were mostly classified as ANME-2c and *Methanosarcinaceae* at the surface, and GoM Arc I (Lloyd et al. 2006) at depth, albeit in low abundance within any of these sediments.

Outside the mat's edge, the methane cyclers of 4486-19 are predominantly *Methanosarcinaceae*, and exceedingly few sequences were recovered from 6-8cmbsf sediments. Just inside the edge of Megamat, in 4486-24, *Methanosarcinaceae* are present at 0-2cmbsf,

19

ANME-2c and GoM Arc I at depth. ANME group sequences comprise less than 15% of >2200 prokaryotic sequences from core 4486-24 at 6-8cm, despite the clear isotopic signatures of sulfate-coupled methane oxidation in these sediments. Of those, most are ANME-2c.

The hottest core 4491-7 hosts deeply-branching "Guaymas Methanomicrobia" sequences (see Figure 15) and ANME-1 groups previously found in high-temperature Guaymas sediments (Biddle et al. 2012, Holler et al. 2011). Core 4491-7 is home to the highest percentage of methanotroph-related sequences. ANME-2c makes up more than 95% of total prokaryotic sequences in 4491-7 surface sediments, while *Methermicoccaceae* turn up at depth, accounting for roughly half of the prokaryotic 16S rRNA sequences recovered from 6-8cmbsf. Guaymas-specific ANME-1 groups may yet represent the most hyperthermophilic, or, at least, most temperature-tolerant methanotrophs known, with RNA still present at *in situ* temperatures exceeding 85ºC. *Methermicoccaceae* and the unstudied "Guaymas Methanomicrobia" clearly play a role in high-temperature Megamat sediments.

3.4   *Archaeal community structure: clone libraries*

Traditional clone libraries were also made with *Archaeal* primers A8f and A1492r, for core 4491-7 and 4486-24 (Figures 16, 17, and 18), to ground-truth the 454 pyrosequencing results presented here. Domain-level *Archaeal* primers appeared to have a bias against Euryarchaeota; phylum-specific primer libraries were therefore also made for 4486-24 to catch a greater diversity of this group, and this small number of bonus clones have been included. The taxonomy in Figure 16 should not be interpreted by any means as absolute abundance, but rather an independent test for the presence or absence of 16S DNA from particular groups. These data nevertheless provide an interesting comparison between both RNA- and DNA-derived full-length 16S sequences and the shorter, RNA-derived pyrosequencing reads.

20

Core 4486-24, at the mat's periphery, returned several full-length sequences of MBGD, MBGB, ANME-2c, and unclassified *Thermoplasmatales*, as in the 454 pyrosequencing library. These primer sets detected members of the Guaymas Euryarchaeotal Group, *Methanomicrobiales*, and *Methanosarcinales* where pyrosequencing did not. Unlike pyrosequencing, the clone libraries did not pick up GoM Arc I or the MCG-15 Group sequences present in this core. In core 4491-7, clone libraries revealed several sequences belonging to the Miscellaneous Crenarchaeotal Group (MCG), DSEV-2 (including the thermoacidophile *Aciduliprofundum*) and *Methanosarcinales*, as did pyrosequencing. These primer sets also detected Thermococcales and members of the Hot Water Crenarchaeotal Group while pyrosequencing did not, but failed to return sequences of *Methanomicrobiaceae* or *Methermicoccaceae* that were prevalent in this sample's 454 pyrosequencing library.

Of those in a small RNA-based clone library for core 4491-7, most reverse-transcribed sequences branched closely to *Aciduliprofundum boonei* (Figure 17) and MCG (Figure 18), with one single clone each near *Thermococcus sibiricus* and in the Hot Water Crenarchaeotal Group. These libraries have the advantage of longer sequence reads and therefore higher-quality alignments. However, the small library size missed a great deal of diversity captured with 454 pyrosequencing.

4. CONCLUSIONS

Guaymas Basin sediments are highly variable even within the context of one individual hydrothermal hot spot, as our Megamat investigation demonstrates. Methane concentration increases in porewater below the central mat, reflected in the high abundance of methane-cycling *Archaea* in these sediments. Sulfate is available at near-seawater concentrations in the surface

layers of all measured sediment cores, but is rapidly depleted with depth in the hottest sediments of Megamat.

OTU abundance was, by far, highest in the surficial sediments outside the perimeter of Megamat (4486-19, 0-2cmbsf), and lowest in the high-temperature, central-mat subsurface (4486-13, 6-8cmbsf). This high-temperature sample had high Shannon-Wiener diversity for total prokaryotes. In surface sediments (0-2cmbsf), *Archaeal* diversity increase linearly with temperature; at 6-8cmbsf, *Archaeal* diversity decreased slightly with temperature, and *Bacterial* diversity decreased in a strongly linear manner with temperature. Temperature appears to influence the community structure, though no doubt its effect is in conjunction with changes in geochemistry across Megamat: for example, higher porewater methane concentrations within central-mat sediments, or lower sulfate concentrations at depth in central-mat sediments, not to mention other possible factors like competition or grazing. Complex combinations of substrate availability, thermal stress, and community interaction likely limit the prokaryotic OTU richness and *Bacterial* diversity within Megamat's subsurface.

Significantly, the community composition across varying thermal and geochemical regimes was remarkably different, in contrast to a recent ARISA-based biogeographic study of Guaymas Basin (Meyer et al. 2013). By contrast to the RNA-based phylogeny presented here, DNA derived diversity may be more similar across disparate Guaymas biogeochemical niches. This study, however, clearly demonstrates a remarkable variety of sequences from the presumably active community over centimeter, decimeter, and meter scales, implying a strong influence of hydrothermal point sources in Guaymas Basin.

The putative sulfur-cycling community was markedly different in high temperature sediments (4486-13, at both 0-2cmbsf and 6-8cmbsf). Few sequences related to those of known

sulfur oxidizers were recovered from the mat's hottest subsurface, unlike other samples presented here (wherein *Sulfurimonas* often dominated the *Bacterial* sequences). *Archaeoglobus* and *Thermodesulfobacteria* dominated these hot sediments both in absolute sequence abundance and percentage of total prokaryotic sequences, by comparison to the handful of *Deltaproteobacteria* recovered in other sediments. *Archaeoglobus* could perhaps be affiliated with high-temperature-tolerant, Guaymas-specific ANME-1, or other anaerobic methane oxidizers, though of course the existing *in-situ* hybridization studies in Guaymas sediments show *Archaeal-Bacterial*, not *Archaeal-Archaeal* partnerships (Teske et al. 2003, Holler et al. 2011, Kellermann et al. 2012). Nevertheless, in light of no *Deltaproteobacterial* sequence recovery within these sediments, high-temperature ANMEs may have a non-proteobacterial partner or no sulfate-reducing partner.

ANME-2c sequences were widespread, even in high-temperature, high porewater methane concentration, low porewater sulfate concentration sediments. ANME-1 Guaymas sequences were only recovered from the hottest sediments (4486-13), and were absent in other high-methane samples. The question of whether ANMEs are separated by temperature, flow, sulfate, oxygen, or other factors in these sediments remains to be fully answered. Deeply-branching Methanomicrobia in these hot sediments beg further exploration. DSEG-3, unclassified *Firmicutes*, and *Thermodesulfobacteria* are also abundant in the highest-temperature sediments presented here, and their role at such high thermal stress relative to local geochemistry is yet to be investigated. RNA recovered from core 4486-13 has experienced temperatures of at least 85°C, among the hottest yet of any successfully-extracted and sequenced RNA.

Prokaryotic community structure was most similar in sediments outside of Megamat, with many majority groups shared between sediments at the mat's edge and in bare sediments

well outside Megamat. Sequences of the heterotrophic MBGB dominate outside of Megamat's perimeters. Within Megamat, cores 4486-13 and 4491-7 had remarkably different community structure, despite their similar porewater methane and sulfate profiles. This may point to the influence of factors like temperature in the mat's subsurface, and highlights niche variability within the mat environment.
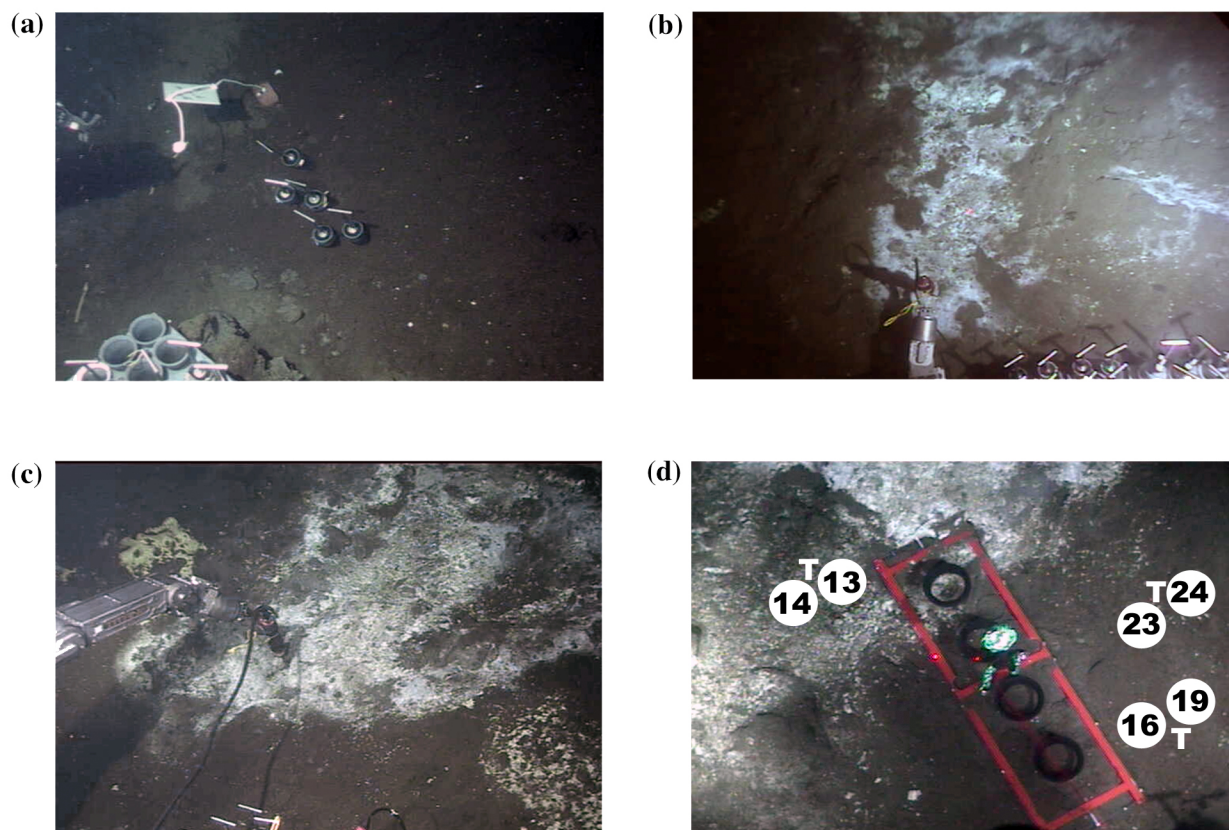
Figure 1: *Context photos of sample areas. (a) Push cores in bare sediment, dive 4485. (b) The far side of Megamat on dive 4491. (c) Alvin's temperature probe in a white portion of mat during dive 4486. (d) Sediment cores taken within the white portion of Megamat and just outside its perimeter. Each black number represents a 4486-X core number, while white "T" indicates point of probe entry for corresponding temperature profiles. (Note the area delineated in red was in place for a separate experiment.)*

a few dozen meters

60 cm

a few meters

5

4

3

2

1

BARE
SEDIMENT

EDGE
OF MAT

CENTRAL
MEGAMAT
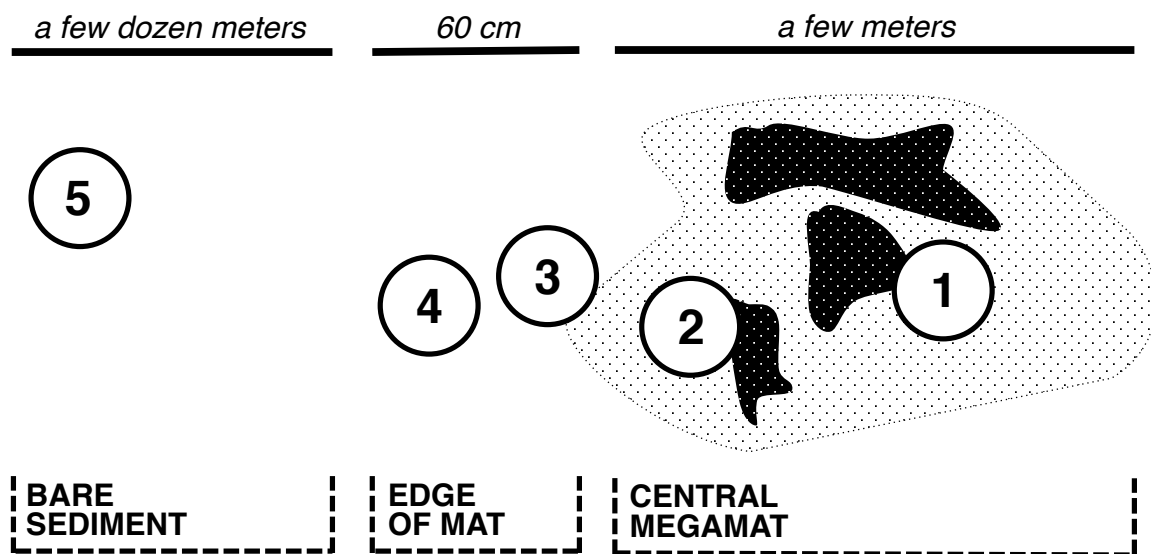
Figure 2: *Cartoon of Megamat and our sample transect. White and orange patches of mat represented by dark and light shaded area. Temperature profiles were collected at these five transect sites, and sediment cores for microbiology and geochemistry were collected as closely as possible to each of those temperature profiles. Core numbers as they will be referred to throughout this manuscript are summarized in Table 1. Note distances in this cartoon are not drawn to scale.*

Table 1: *Summary of coordinating sediment cores and closest in situ temperature measurement*

Environment	Transect Site (*Figure 2*)	Molecular biology core	Geochemistry core	*In situ* temperature (ºC)		
				(0-2 cmbsf)	(6-8 cmbsf)	(40-42 cmbsf)
Bare sediment	5	4485-5	4485-1	3	3	3
Edge of Megamat	4	4486-19	4486-16	11	32	84
	3	4486-22	4486-24	10	34	101
Central Megamat	2	4486-13	4486-14	26	85	163
	1	4491-7	4491-12	6	19	112

Table 2: *Summary of amplified cDNA concentration and final volume sent for pyrosequencing.*

Environment	Molecular Biology Core	Sediment Subsection (cmbsf)	Amplified cDNA Concentration (ng/µl)	Final Volume (µl)
Bare sediment	4485-5	0-2	16.6	10
		6-8	10.9	14
Edge of Megamat	4486-19	0-2	13.2	12
		6-8	10.7	15
	4486-22	0-2	14.4	11
		6-8	6.4	18
Central Megamat	4486-13	0-2	10.4	15
		6-8	9.3	17
	4491-7	0-2	16.2	10
		6-8	12.4	13
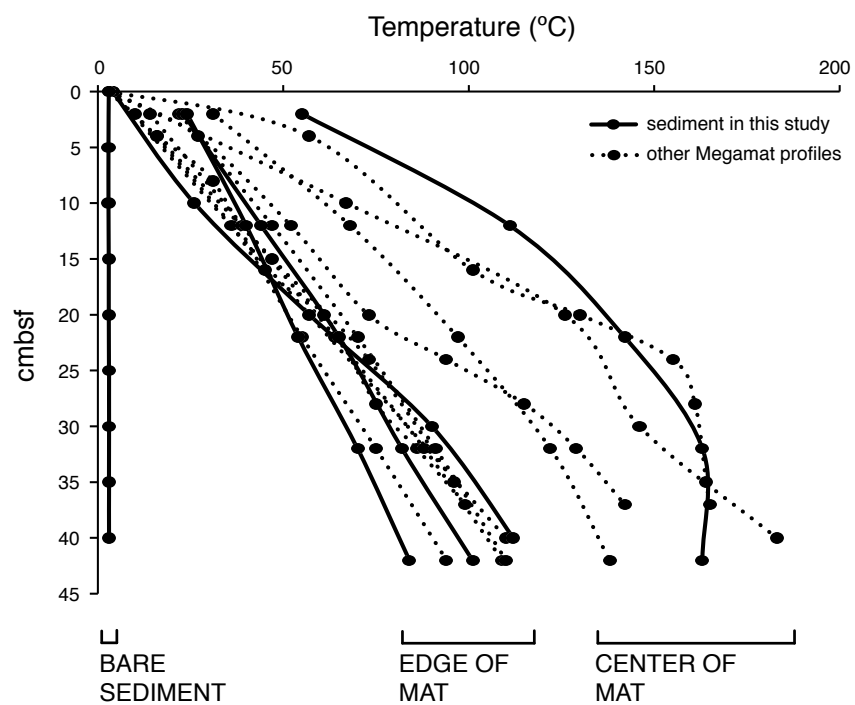
Figure 3: *Subsurface temperatures within Megamat (and bare sediment, several dozen meters away). Solid lines represent cores used in this study; dotted lines are profiles also taken within mat-covered sediments ("center of mat") or just outside its perimeter ("edge of mat").*

Figure 4: *Geochemical and temperature profiles of Megamat.*

(a) BARE SEDIMENT
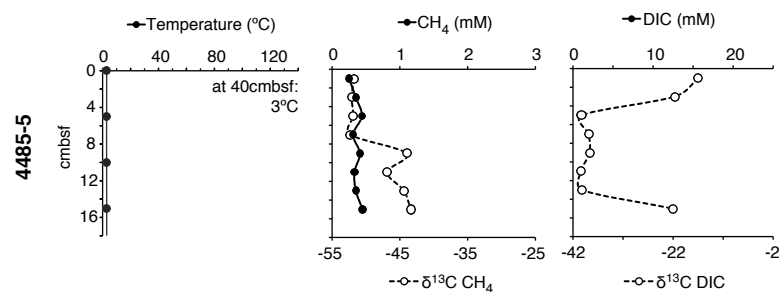
(b) EDGE OF MEGAMAT
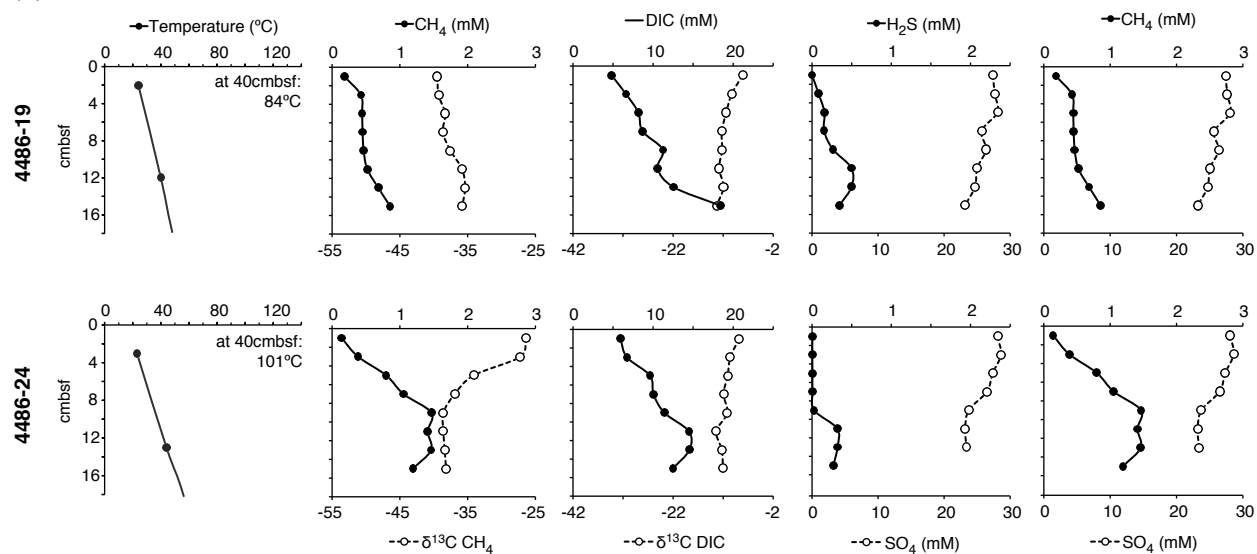
(c) CENTRAL MEGAMAT
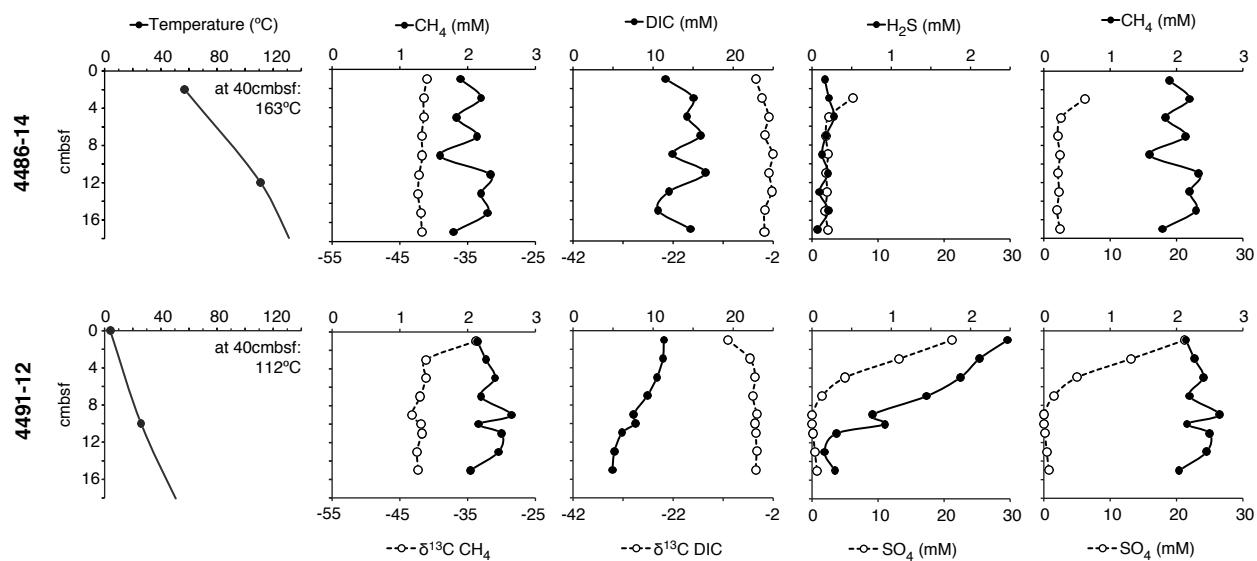
Table 3: *Summary of 454 pyrosequencing reads per sample.*

Depth		0-2cm					6-8cm				
Environment		Bare Sediment	Edge of Megamat		Central Megamat		Bare Sediment	Edge of Megamat		Central Megamat	
Microbiology Core		4485-5	4486-19	4484-24	4486-13	4491-7	4485-5	4486-19	4484-24	4486-13	4491-7
Total Reads		2699	4641	2504	3005	3406	3398	3541	2210	1526	2621
Domain-Level Reads	Archaea	1876	4361	2343	2585	2487	2799	3507	2101	1091	2302
	Bacteria	823	280	161	420	919	599	34	109	435	319
Arch:Bac Ratio		2.3	15.6	14.6	6.2	2.7	4.7	103.2	19.3	2.5	7.2
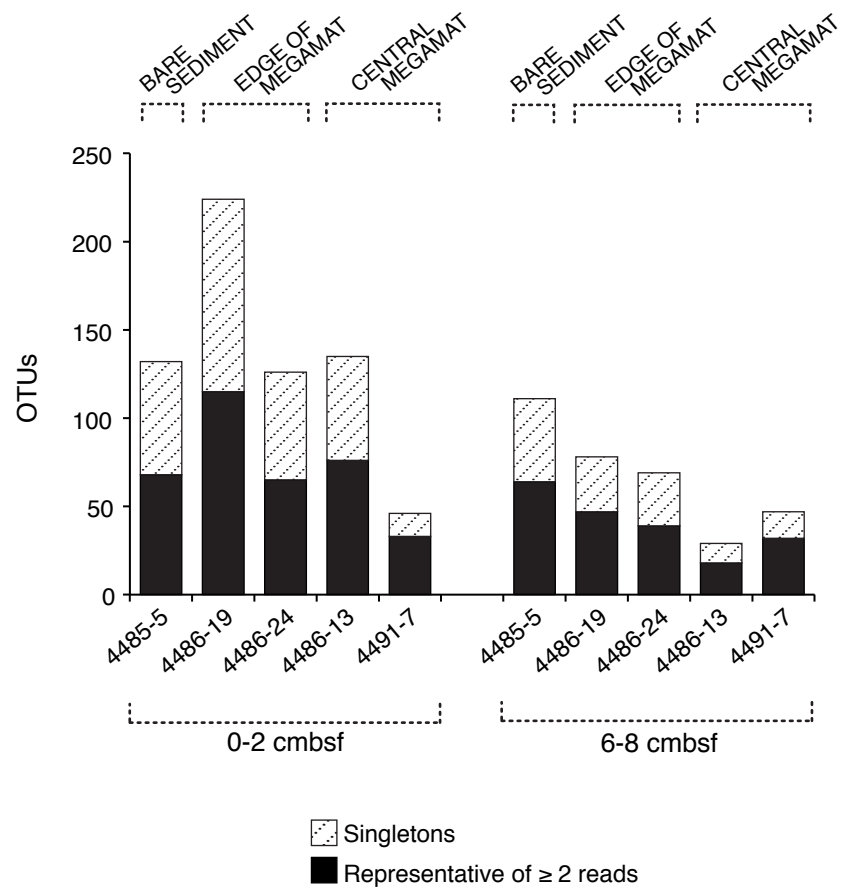
Figure 5: *OTU abundance per sample. OTUs representative of single reads are shown in light shading, while OTUs representative of multiple reads are shown in black.*
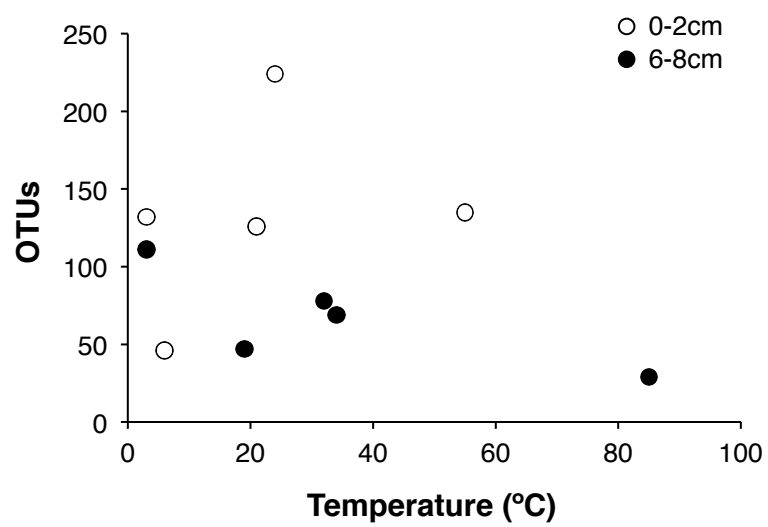
Figure 6: *Number of OTUs per sample vs. temperature, separated by sample depth (cmbsf)*
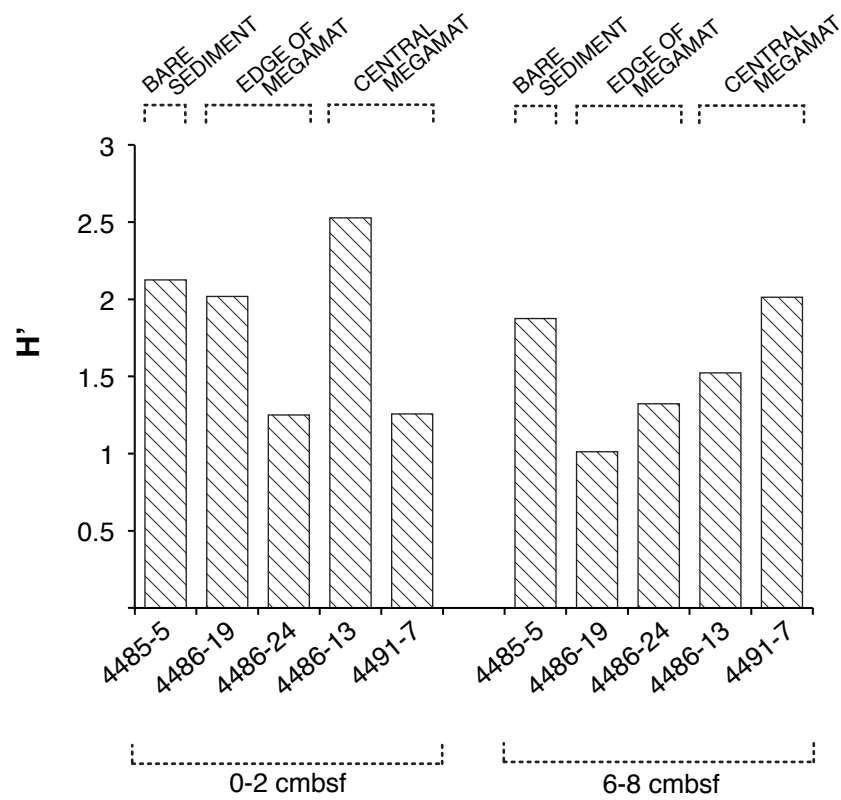
Figure 7: *Shannon-Wiener diversity (H') of total prokaryotic community per sample.*
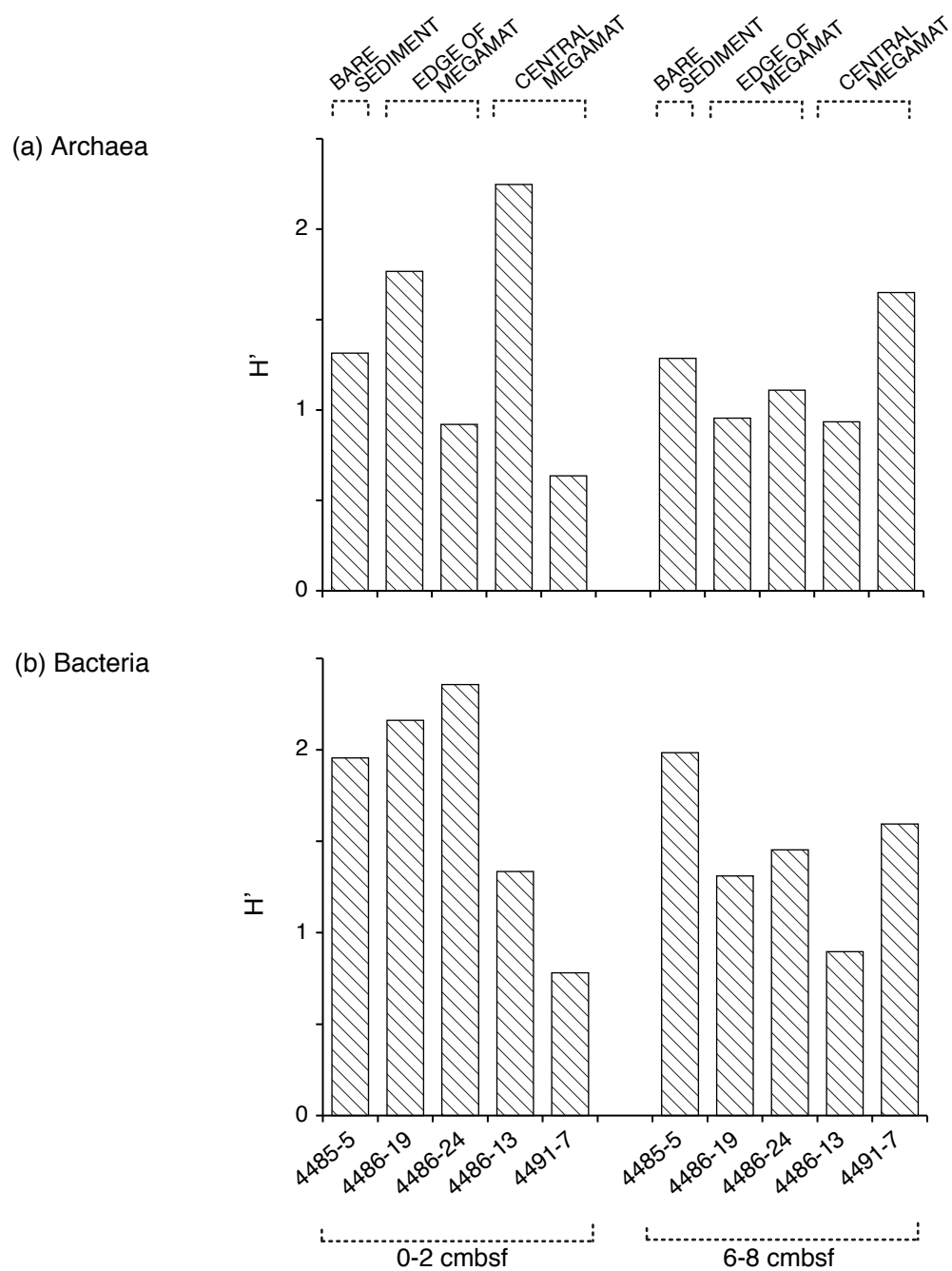
Figure 8: *Shannon-Wiener diversity (H') per sample for (a) Archaea and (b) Bacteria*
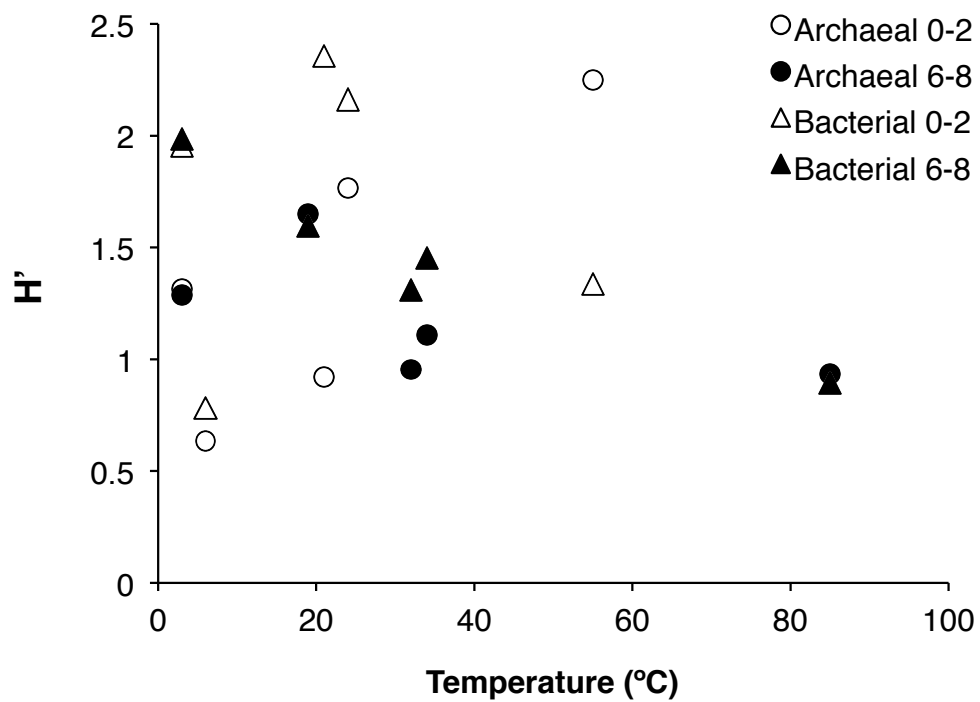
Figure 9: *Domain-level Shannon-Wiener diversity (H') vs. temperature, separated by Archaea (circles) and Bacteria (triangles) and by depth (0-2cmbsf, white, or 6-8cmbsf, black).*

(a) ARCHAEAL COMMUNITY COMPOSITION

36
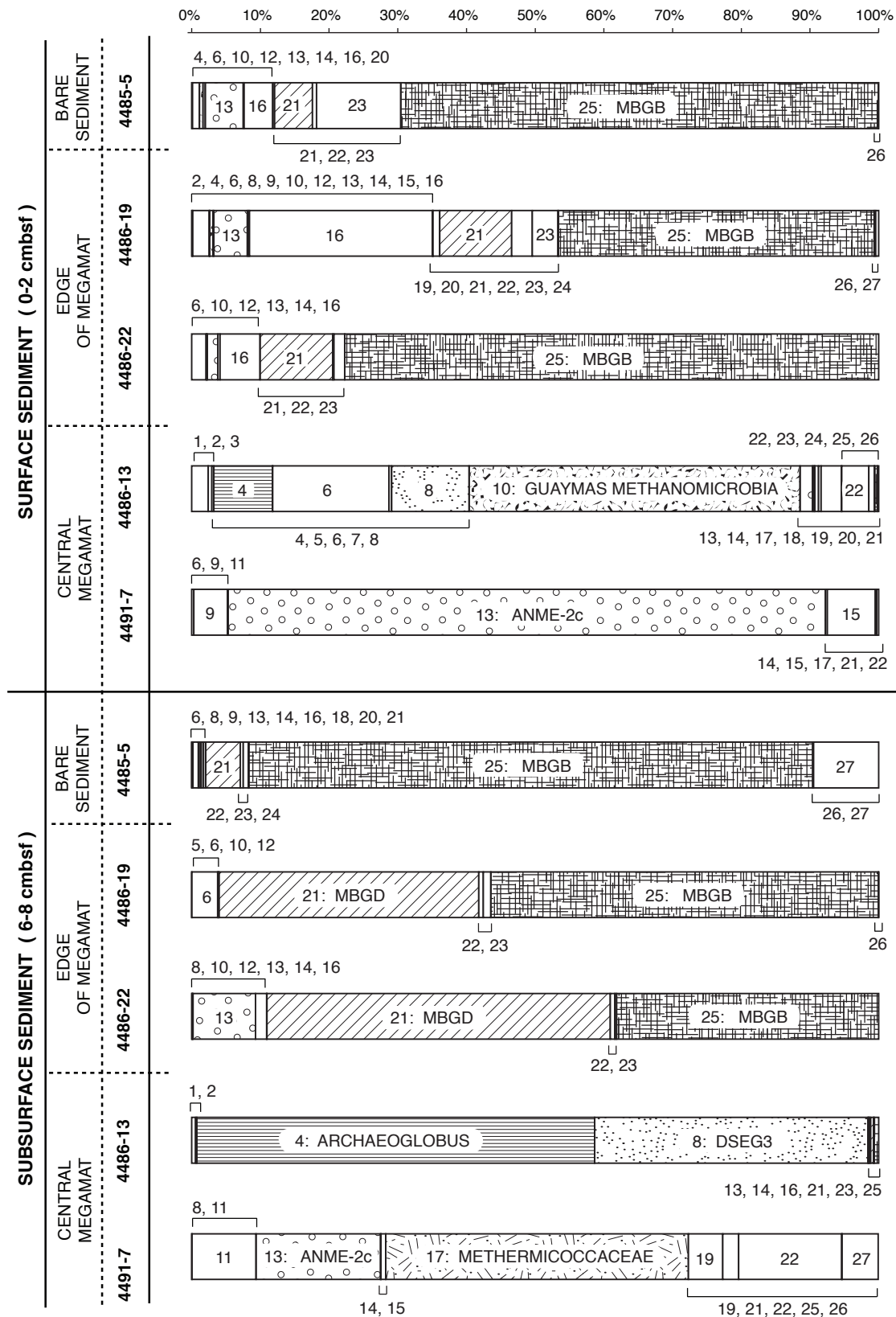
(b) BACTERIAL COMMUNITY COMPOSITION
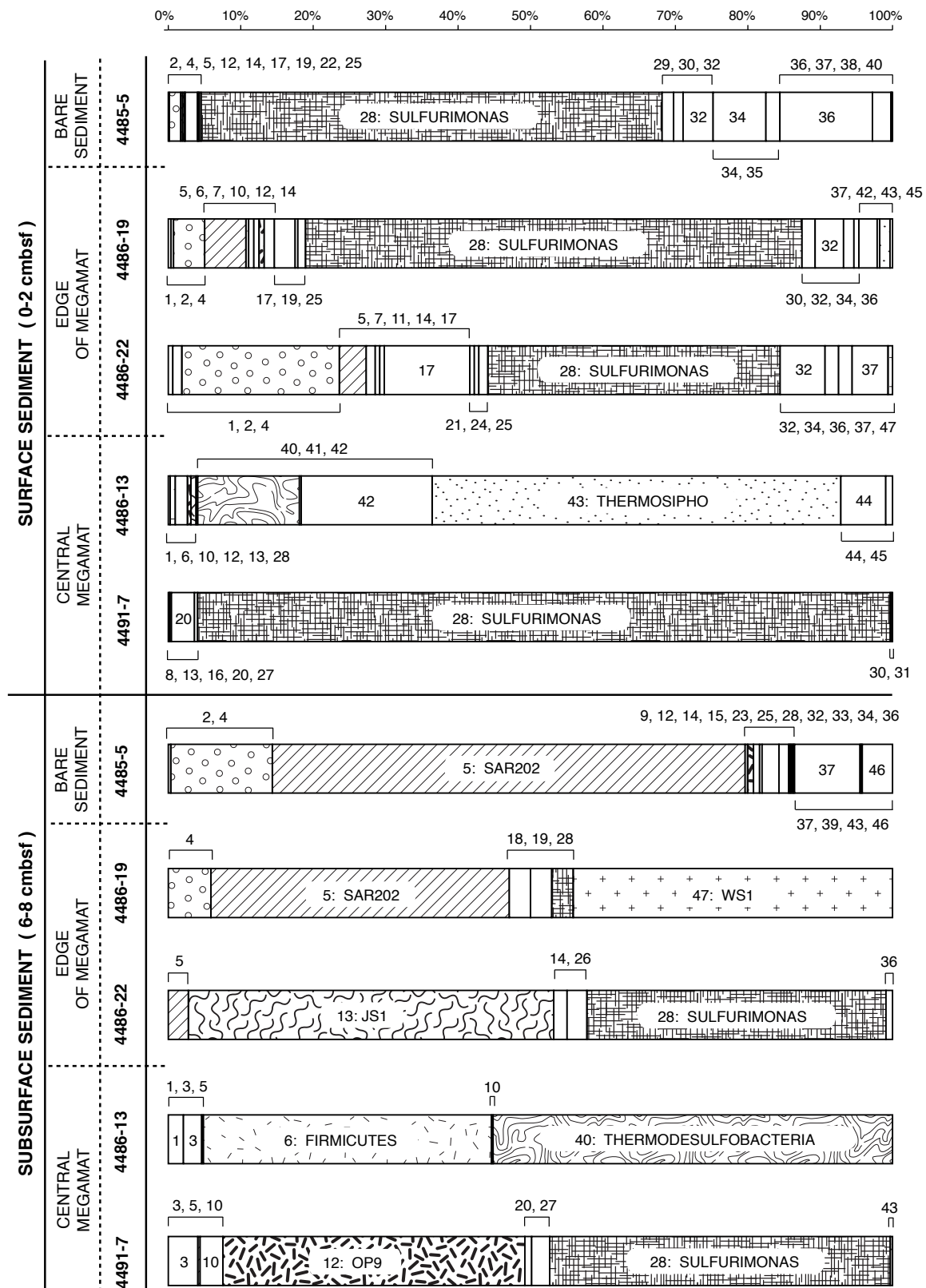
(c) LEGEND
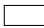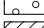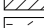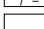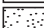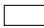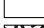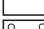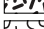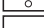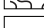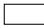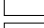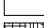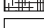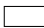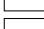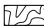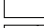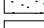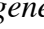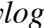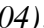
ARCHAEA		BACTERIA	
1	ANME-1 Guaymas	1	Acidobacteria
2	ANME-1 Guaymas II	2	Bacteroidetes
3	ANME-1a	3	Aerophobetes
4	Archaeoglobus	4	Dehalococcoides
5	Other Archaeoglobaceae	5	SAR202
6	DHVE-6	6	Firmicutes
7	DHVE-8	7	Psychrilyobacter
8	DSEG-3	8	Hyd24-12
9	Microarchaeum	9	Lentisphaerae
10	Guaymas Methanomicrobia	10	OP1
11	Methanomicrobiaceae	11	OP3
12	ANME-2b	12	OP9
13	ANME-2c	13	JS1
14	GoM Arc I	14	Planctomycetaceae
15	Methanosaeta	15	Magnetospira
16	Methanosarcinaceae	16	Desulfobacter
17	Methermicoccaceae	17	Desulfobacterium
18	Guaymas Euryarchaeotal Group	18	Desulfococcus
19	Aciduliprofundum	19	Desulfonema
20	DHVE-1	20	Other Desulfobacteraceae
21	MBGD	21	Desulfobulbus
22	Other Thermoplasmatales	22	Desulfocapsa
23	MCG-15	23	Nitrospina
24	MBGA	24	Desulfuromonas
25	MBGB	25	Sva0853
26	MCG	26	Desulfobacca
27	MG-I	27	Desulfomonile
		28	Sulfurimonas
		29	Colwellia
		30	Moritella
		31	Pseudoalteromonas
		32	Psychromonas
		33	Chromatiales
		34	Methylococcaceae
		35	Oceanospirillaceae
		36	Cycloclasticus
		37	Uncultured Gammaproteobacteria
		38	Marinicella
		39	Spirochaetes
		40	Thermodesulfobacteria
		41	Geotoga
		42	Marinitoga
		43	Thermosipho
		44	Thermotoga
		45	Other Thermotogales
		46	Verrucomicrobiaceae
		47	WS1

Figure 10: *(a) Archaeal and (b) Bacterial phylogenetic assignments at as specific a taxonomic designation as possible, with legend (c). This phylogeny is based on alignments and neighbor-joining trees constructed in Arb (Ludwig et al. 2004). Only bootstrap confidence values >50% are shown. Major groups are indicated by patterns, minor groups by white fill. All groups have a number designation (see legend). Note groups are not all at the same taxonomic level.*
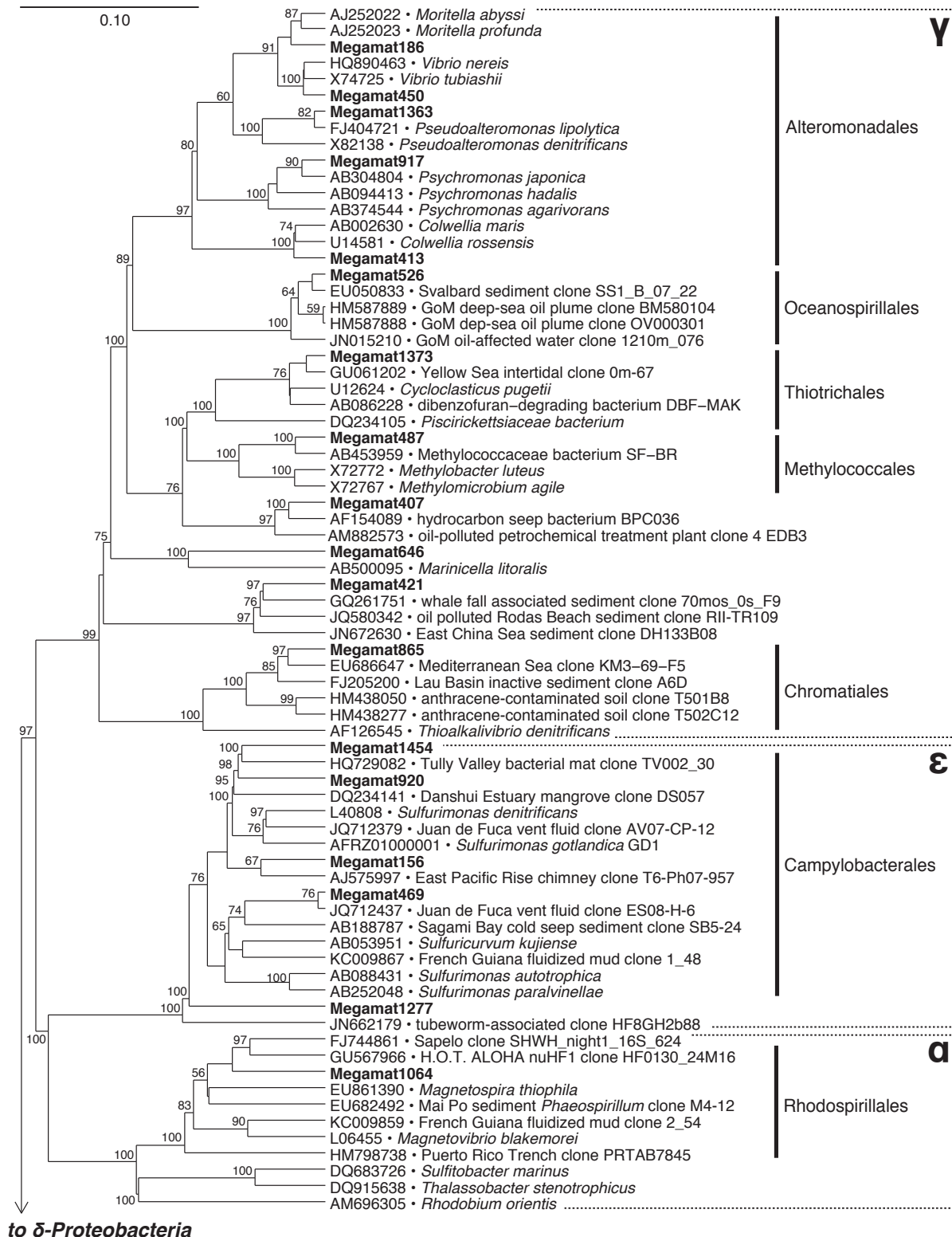
Figure 11: *Phylogenetic lineages of Proteobacteria, excluding Deltaproteobacteria (see Figure 13). Neighbor-joining phylogeny based on the V5-V8 region, approximately 600bp. Built with Arb software (Ludwig et al. 2004). Bootstrap support for nodes >50% are shown.*
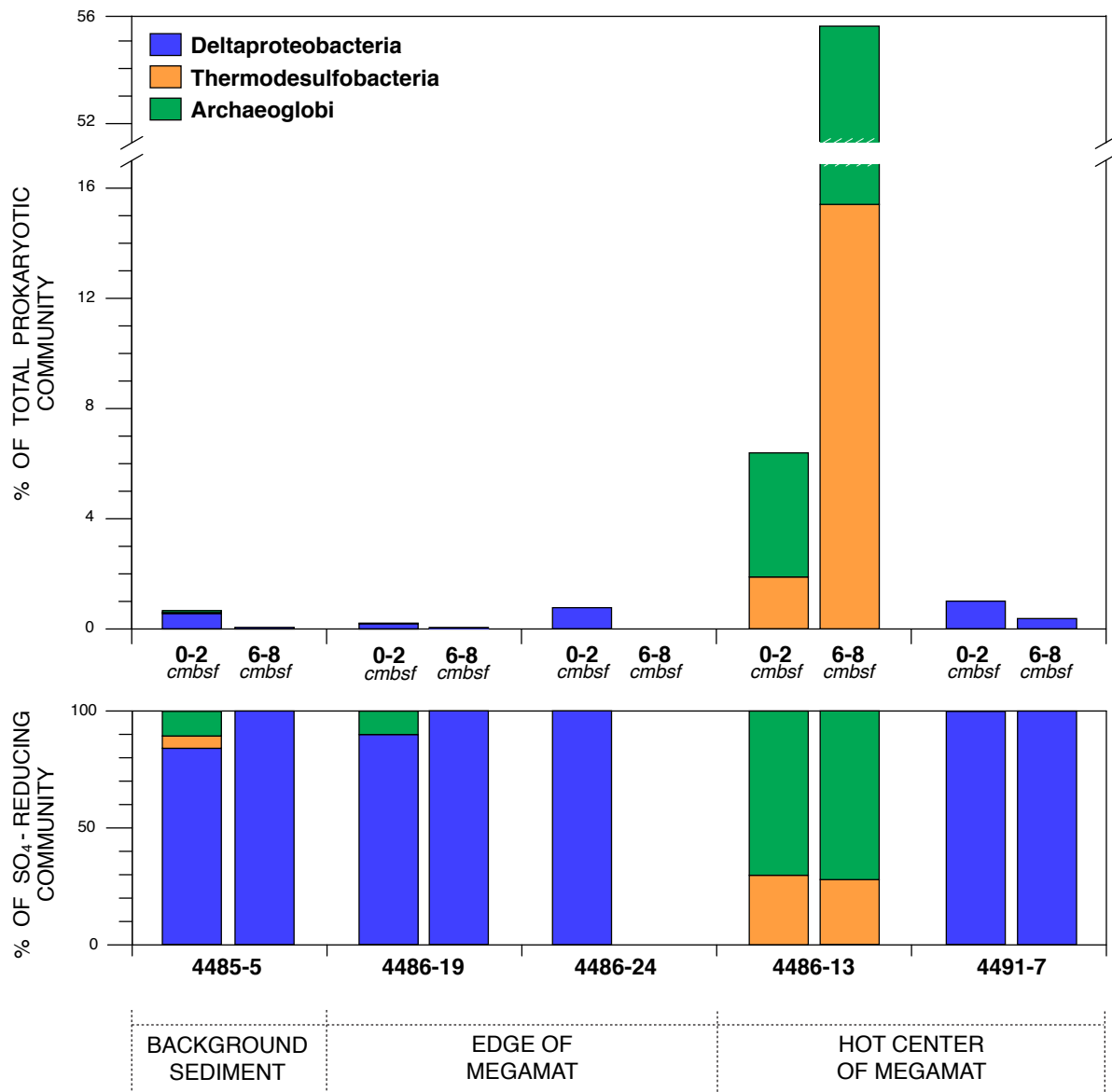
Figure 12: *Proportional representation of known sulfate-reducing lineages in the pyrosequencing dataset. The top portion of this figure shows abundance of Deltaproteobacteria, Thermodesulfobacteria, and Archaeoglobi as a percentage of the total community sequenced per sediment section, while the bottom portion shows these communities normalized to 100% of the sulfate-reducers present in each sample. Taxonomic designations inferred from neighbor-joining trees constructed in Arb (Ludwig et al. 2004). Note the break from 17-51% in the upper y-axis.*

Figure 13: *Neighbor-joining tree of sulfate-reducing and related sequences from Megamat, with a heat plot of sequence abundance per sample. Shaded boxes indicate sequence presence; black boxes indicate dominance of those sequences in a sample. Bootstraps >50% are shown.*

41
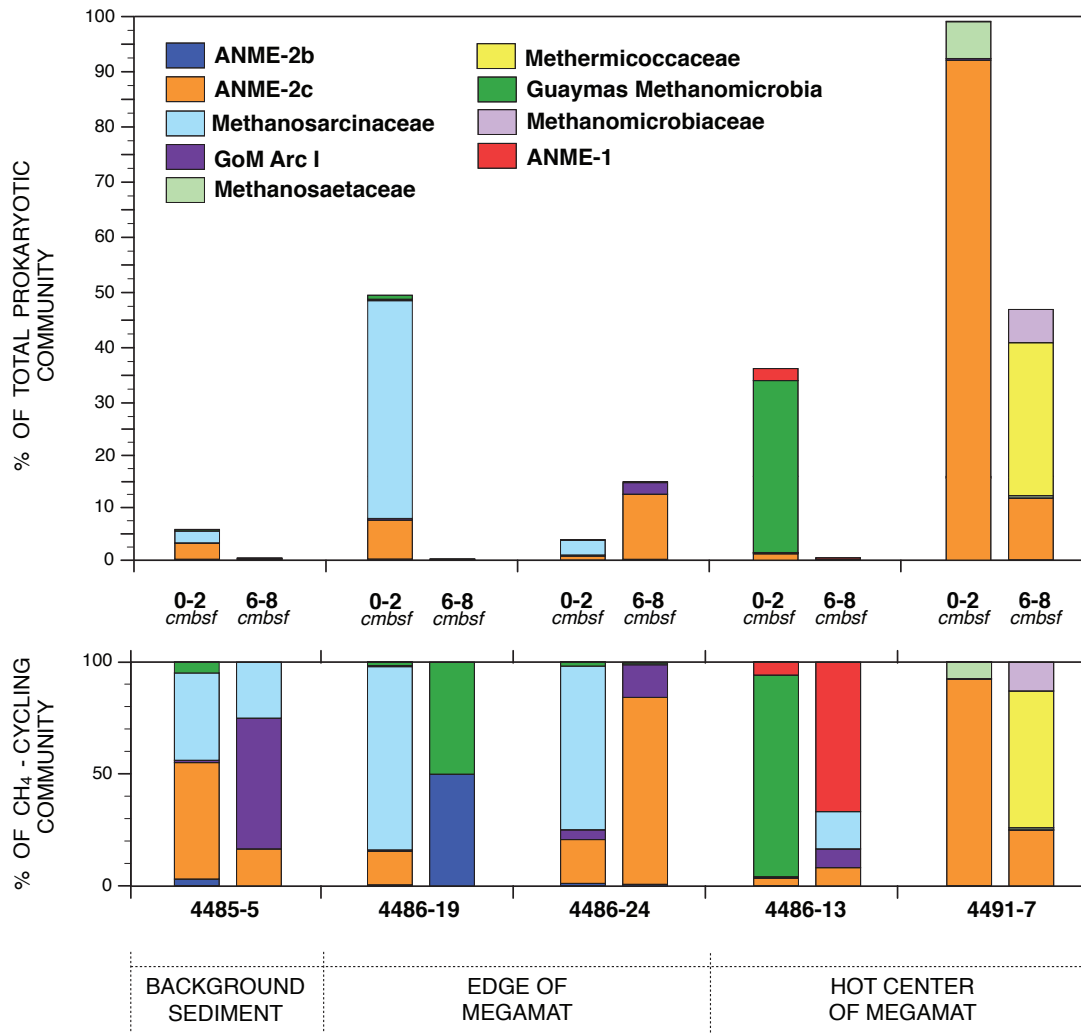
Figure 14: *Proportional representation of methanogenic and methane-oxidizing Archaea in the pyrosequencing dataset, as a percentage of total prokaryotic community (top) and normalized within each sample (bottom). Note the red ANME-1 bars encompass ANME-1a, ANME-1b, ANME-1 Guaymas, and ANME-1 Guaymas II (see Figure 15).*

Figure 15: *Neighbor-joining tree of known methanogens, methanotrophs, and related; heat plot with shaded scheme as in Figure 13. Bootstraps >50% are shown.*

EDGE OF MAT (4486-24)

CENTRAL MEGAMAT (4491-7)

Figure 16: *Clone-library based phylogeny of two Megamat samples, both from 6-8cmbsf.*

100 — **4486-22 6–8 Arch DNA071 (1 clone)**
95 — **4486-22 6–8 Eury 029 (2 clones)**
73 — DQ522923 • Skan Bay clone SBAK–mid–25
DQ522921 • Skan Bay clone SBAK–mid–19
95 — **4486-22 6–8 Arch DNA080 (1 clone)**
80 — AF015992 • Saltmarsh clone 2MT8
100 — **4486-22 6–8 Arch DNA072 (1 clone)**
AF134389 • marine sediment clone TA1e6
73 — **4486-22 6–8 Arch DNA093 (8 clones)**
DQ640154 • Skan Bay clone SBAK–shallow–01
4486-22 6–8 Eury DNA016 (1 clone)
80 — **4486-22 6–8 Arch DNA069 (1 clone)**
AJ969751 • soil clone ss012
95 — **4486-22 6–8 Arch DNA065 (4 clones)**
100 — EF051157 • mangrove sediment clone XMA60
4486-22 6–8 Arch DNA094 (1 clone)
80 — **4486-22 6–8 Arch DNA081 (1 clone)**
AF119123 • deep-sea sediment clone CRA12–27cm
95 — 100 — AB177285 • Pacific Ocean Margin clone ODP1251A3.9
95 — AF015981 • Saltmarsh clone 2MT1
98 — **4486-22 6–8 Arch DNA070 (1 clone)**
99 — AF050619 • aquifer clone WCHD3–33
98 — AY835423 • Guaymas Basin clone 7C08
79 — **4486-22 6–8 Arch DNA054 (1 clone)**
77 — AB237748 • aquifer clone HDBW–WA15
AY835424 • Guaymas Basin clone 1E11

MARINE BENTHIC GROUP D

THERMOPLASMATALES -RELATED

74 —
73 — **4491-7 7–8 DNA31 (19 clones)**
4491-7 7–8 RNA42 (26 clones)
95 — DQ451875 • *Aciduliprofundum boonei*
99 — AB019739 • hydrothermal vent clone pMC2A10 .... DSVE 2
100 — AB269873 • *Thermogymnomonas acidicola*
M38637 • *Thermoplasma acidophilum*

95 — **4491-7 7–8 DNA11 (2 clones)**
92 — AY835418 • Guaymas Basin clone 1E10
82 — AY817738 • *Methanosaeta harundinacea*
95 — **4486-22 6–8 Arch DNA062 (3 clones)**
100 — **4486-22 6–8 Eury DNA003 (1 clone)**
99 — X65537 • *Methanococcoides burtonii*
73 — M59133 • *Methanohalophilus mahii*
79 — AF028691 • *Methanosarcina mazei*
4486-22 6–8 Arch DNA092 (1 clone)
95 — AJ578128 • Black Sea cold seep clone BS–K–H6
100 — AF354134 • Santa Barbara Basin clone SB-24a1F10
95 — AF354128 • Eel River Basin clone Eel-36a2A4
95 — **4486-22 6–8 Arch DNA024 (7 clones)**
AF354131 • Santa Barbara Basin clone SB-24a1A12
73 — AF419638 • Guaymas Basin clone C1 R019
95 — AF419647 • Guaymas Basin clone CS R012
AF354129 • Eel River Basin clone Eel-36a2A1

ANME 2ab

ANME 2c

METHANOSARCINALES

97 — **4486-22 6–8 Arch DNA064 (1 clone)**
69 — AJ578125 • Black Sea clone BS–K–E9
95 — **4486-22 6–8 Eury DNA005 (1 clone)**
AF050620 • aquifer clone WCHD3–34
73 — M59142, *Methanomicrobium mobile*
95 — AB065297, *Methanoculleus thermophilus* .... METHANOMICROBIALES

100 — **4486-22 6–8 Arch DNA075 (1 clone)**
100 — AY592838 • mud volcano clone Milano–WF2A–14
60 — AY835427 • Guaymas Basin clone 4E09
99 — AF050614 • aquifer clone WCHA1–57
100 — AY835425 • Guaymas Basin clone 4D08
AF419629 • Guaymas Basin clone A2 B037

GUAYMAS EURYARCHAEOTAL GROUP

97 — AY196675 • *Methanococcus vannielii*
L77117 • *Methanocaldococcus jannaschii*
100 — **4491-7 7–8 DNA02 (6 clones)**
100 — **4491-7 7–8 RNA33 (1 clone)**
100 — AJ238992 • *Thermococcus sibiricus*
72 — AE010139 • *Pyrococcus furiosus* .... THERMOCOCCALES
AJ299219 • *Archaeoglobus profundus*
100 — M36474 • *Desulfurococcus mobilis*
95 — AB029339 • *Pyrobaculum oguniense*
X14835 • *Thermofilum pendens*

98 —
82 —
99 —
100 —

0.10

Figure 17: *Neighbor-joining tree of Euryarchaeotal clone libraries. Clones with "RNA" in their name are from RNA extractions, "DNA" from DNA extractions. Clones named with "Arch" were amplified using domain-level PCR primers, while "Eury" were amplified with Euryarchaeotal-specific primers.*

45
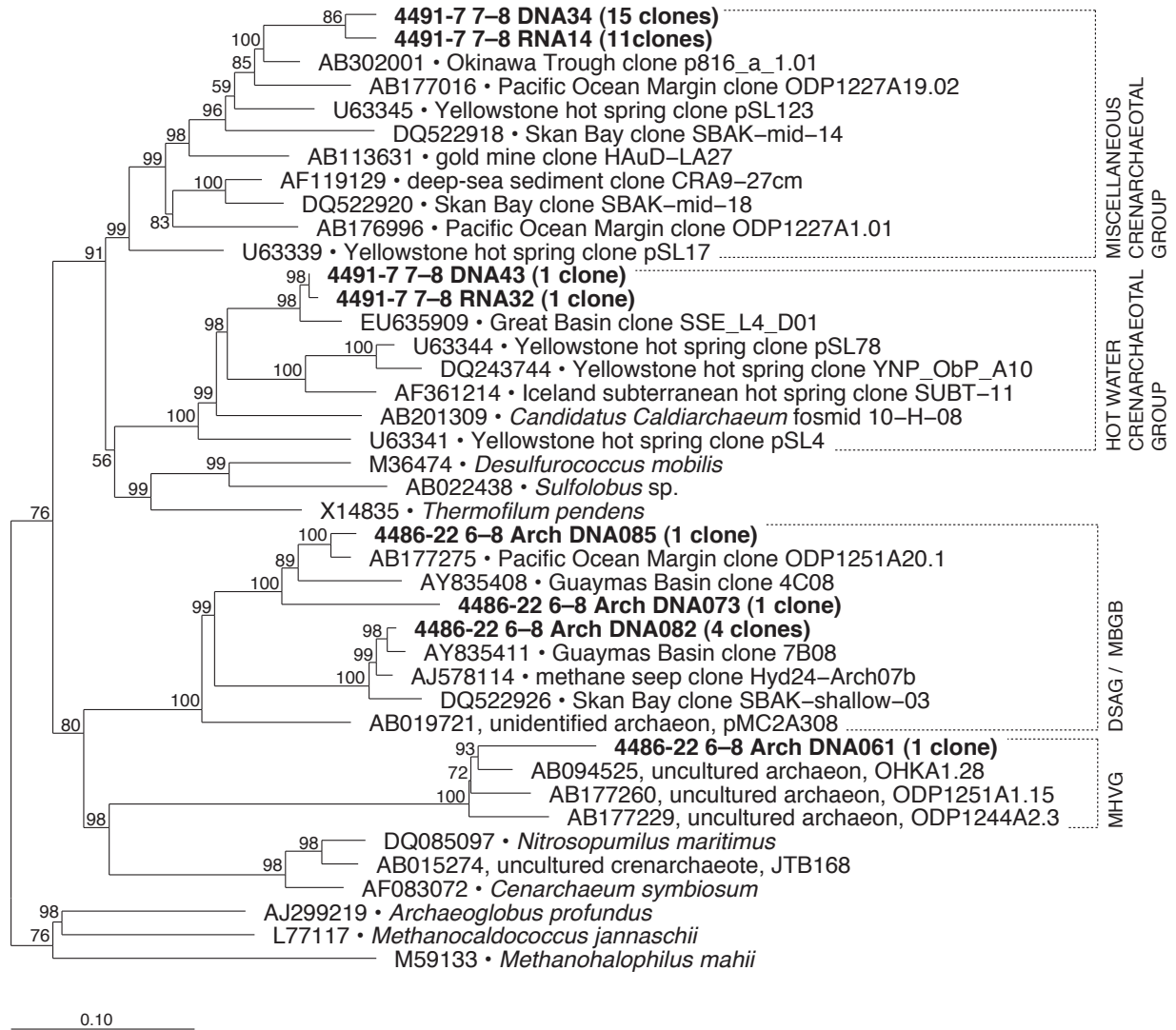
Figure 18: *Crenarchaeotal phylogeny from full-length 16S clone libraries. "DNA" and "RNA" denote the same distinction as in Figure 17; all clones in this neighbor-joining tree were amplified using domain-level Archaeal primers.*

REFERENCES

Auguet J.-C., Barberan A., and Casamayor E. O. (2010) Global ecological patterns in uncultured Archaea. *The ISME Journal* 4: 182-190.

Baker B. J., Tyson G. W., Webb R. I., Flanagan J., Hugenholtz P., Allen E. E., and Banfield J. F. (2006). Lineages of acidophilic Archaea revealed by community genomic analysis. *Science* 314: 1933-1935.

Biddle J. F., Lipp J. S., Lever M. A., Lloyd K. G., Sørensen K. B., Anderson R., Fredericks H. F., Elvert M., Kelly T. J., Schrag D. P., Sogin M. L., Brenchley J. E., Teske A., House C. H., and Hinrichs K. U. (2006) Heterotrophic Archaea dominate sedimentary subsurface ecosystems off Peru. *Proceedings of the National Academy of Sciences of the United States of America* 103(10): 3846-3851.

Biddle J. F., Cardman Z., Mendlovitz H., Albert D. B., Lloyd K. G., Boetius A., and Teske A. (2012) Anaerobic oxidation of methane at different temperature regimes in Guaymas Basin hydrothermal sediments. *The ISME Journal* 6(5): 1018-1031.

Burggraf S., Mayer T., Amann R., Schadhauser S., Woese C. R., and Stetter K. O. (1994) Identifying members of the domain Archaea with ribosomal-RNA-targeted oligonucleotide probes. *Applied and Environmental Microbiology* 60: 3112-3119.

Calvert S. E. (1966) Origin of diatom-rich, varved sediments from the Gulf of California. *Journal of Geology* 74(5): 546-565.

Campbell B. J. and Kirchman D. (2013) Bacterial diversity, community structure and potential growth rates along as estuarine salinity gradient. *The ISME Journal* 7, 210-220.

Campbell B. J., Engel A. S., Porter M. L. and Takai K. (2006). The versatile epsilonproteobacteria: key players in sulphidic habitats. *Nature Reviews Microbiology* 4: 458-468.

Cline J. D. (1969). Spectrophotometric determination of hydrogen sulfide in natural waters. *Limnology and Oceanography* 14, 454–458.

Dell'Anno A. and Danovaro R. (2005) Extracellular DNA plays a key role in deep-sea ecosystem functioning. *Science* 309 (5744), 2179

Dhillon, A., Teske A., Dillon J., Stahl D. A., and Sogin M. L. (2003) Molecular characterization of sulfate-reducing bacteria in the Guaymas Basin. *Applied and Environmental Microbiology* 69:2765-2772

Dhillon, A., Lever M., Lloyd K., Albert D. B., Sogin M. L., and Teske A. (2005) Methanogen diversity evidenced by molecular characterization of methyl coenzyme M reductase A

(mcrA) genes (*mcr*A) in hydrothermal sediments of the Guaymas Basin. *Applied and Environmental Microbiology* 71:4592-4601.

Einsele G., Gieskes J. M., Curray J., Moore D. M., Aguayo E., Aubry M.-P., Fornari D., Guerrero J., Kastner M., Kelts K., Lyle M., Matoba Y., Molina-Cruz A., Niemitz J., Rueda J., Saunders A., Schrader H., Simoneit B., and Vacquier V. (1980) Intrusion of basaltic sills into highly porous sediments, and resulting hydrothermal activity. *Nature* 283: 441 – 445.

Felsenstein J. (1985) Confidence limits on phylogenies: an approach using the bootstrap. *Evolution* 39(4): 783-791.

Gundersen J. K., Jørgensen B. B., Larsen E., Jannasch H. W. (1992) Mats of giant sulphur bacteria on deep-sea sediments due to fluctuating hydrothermal flow. *Nature* 360: 454 – 456

Heijs S. K., Haese R. R., van der Wielen P. W. J. J., Forney L. J., and van Elsas J. D. (2007) Use of 16S rRNA gene based clone libraries to assess microbial communities potentially involved in anaerobic methane oxidation in a Mediterranean cold seep. *Microbial Ecology* 53(3): 384-398.

Hill T. C. J., Walsh, K. A., Harris, J. A., and Moffett B. F. (2003) Using ecological diversity measures with bacterial communities. *FEMS Microbiology* 43: 1-11.

Holler, T. F. Widdel, K. Knittel, R. Amann, M. Y. Kellermann, K.-. Hinrichs, A. Teske, A. Boetius, and G. Wegener. (2011) Thermophilic anaerobic oxidation of methane by marine microbial consortia. *The ISME Journal* 5:1946-1956.

Inagaki, F., Nunoura T., Nakagawa S., Teske A., Lever M. A., Lauer A., Suzuki M., Takai K., Delwiche M., Colwell F. S., Nealson K. H., Horikoshi K., D'Hondt S. L., and Jørgensen B. B. (2006) Biogeographical distribution and diversity of microbes in methane hydrate-bearing deep marine sediments on the Pacific Ocean Margin. *Proceedings of the National Academy of Sciences of the United States of America* 103: 2815-2820.

Jannasch, H. W., Nelson, D. C., and Wirsen, C. O. (1989) Massive natural occurrence of unusually large bacteria (*Beggiatoa* sp.) at a hydrothermal deep-sea vent site. *Nature* 342: 834–836.

Jørgensen S. L., Hannisdal B., Lanzén A., Baumberger T., Flesland K., Fonesca R., Ovreas L., Steen I. H., Thorseth I. H., Pedersen R. B., and Schleper C. (2012) Correlating microbial community profiles with geochemical data in highly stratified sediments from the Arctic Mid-Ocean Ridge. *Proceedings of the National Academy of Sciences of the United States of America* 109(42): E2846-2855.

Kawka O. E. and Simoneit B. R. T. (1987) Survey of hydrothermally-generated petroleums from the Guaymas Basin spreading center. *Organic Geochemistry* 11(4): 311-328.

Kellermann M., Wegener G., Elvert M., Yoshinaga M. Y., Lin Y.-S., Holler T., Mollar X. P., Knittel K., and Hinrichs K.-U. (2012) Autotrophy as a predominant mode of carbon fixation in anaerobic methane-oxidizing microbial communities. *Proceedings of the National Academy of Sciences of the United States of America* 109:19321-19326

Klenk H. P., Clayton R. A., Tomb J.-F., White O., Nelson K. E., Ketchum K. A., Dodson R. J., Gwinn M., Hickey E. K., Peterson J. D., Richardson D. L., Kerlavage A. R., Graham D. E., Kyrpides N. C., Fleishmann R. D., Quackenbush J., Lee N. H., Sutton G. G., Gill S., Kirkness E. F., Dougherty B. A., McKenny K., Adams M. D., Loftus B., Peterson S., Reich C. I., McNeil L. K., Badger J. H., Glodek A., Zhou L., Overbeek R., Gocayne J. D., Weidman J. F., McDonald L., Utterback T., Cotton M. D., Spriggs T., Artiach P., Kaine B. P., Sykes S. M., Sadow P. W., D'Andrea K. P., Bowman C., Fujii C., Garland S. A., Mason T. M., Olsen G. J., Fraser C. M., Smith H. O., Woese C. R., and Venter J. C. (1997). The complete genome sequence of the hyperthermophilic, sulphate-reducing archaeon *Archaeoglobus fulgidus*. *Nature* 390: 364-370.

Knittel K., Boetius A., Lemke A., Eilers H., Lochte K., Pfannkuche O., Linke P., and Amann R. (2003) Activity, distribution, and diversity of sulfate reducers and other bacteria in sediments above gas hydrate (Cascadia Margin, OR). *Geomicrobiology Journal* 20: 369-294.

Knittel K., Lösekann T., Boetius A., Kort R., and Amann R. (2005) Diversity and Distribution of Methanotrophic Archaea at Cold Seeps. *Applied and Environmental Microbiology* 71(1): 467 – 479.

Kysela D. T., Palacios C., and Sogin M. L. (2005). Serial analysis of V6 ribosomal sequence tags (SARST-V6): a method for efficient, high-throughput analysis of microbial community composition. *Environmental Microbiology* 7, 356–364.

Lane D. J., Pace B., Olsen G. J., Stahl D. A., Sogin M. L., and Pace N. R. (1985) Rapid determination of 16S ribosomal RNA sequences for phylogenetic analyses. *Proceedings of the National Academy of Sciences of the United States of America* 82:6955–6959

Lizarralde D., Soule S. A., Seewald J. S., and Proskurowski G. (2011). Carbon release by off-axis magmatism in a young sedimented spreading centre. *Nature Geoscience* 4: 50-54.

Lloyd K.G., Lapham L., and Teske A. (2006) An anaerobic methane-oxidizing community of ANME-1 archaea in hypersaline Gulf of Mexico sediments. *Applied and Environmental Microbiology* 72:7218-7230

Lloyd K.G., Albert D.B., Biddle J.F., Chanton J.P., Pizarro O., and Teske A. (2010) Spatial Structure and Activity of Sedimentary Microbial Communities Underlying a *Beggiatoa* spp. Mat in a Gulf of Mexico Hydrocarbon Seep. *PLoS ONE* 5(1): e8738.

Lloyd, K. G., Alperin M., and Teske A. (2011) Environmental evidence for net methane production and oxidation in putative Anaerobic MEthanotrophic (ANME) archaea. *Environmental Microbiology* 13: 2548-2564

Lonsdale P., and Becker K. (1985) Hydrothermal plumes, hot springs, and conductive heat flow in the Southern trough of the Guaymas Basin. *Earth and Planetary Science* 73: 211-225.

Ludwig W., Strunk O., Westram R., Richter L., Meier H., Yadhukumar, Buchner A., Lai T., Steppi S., Jobb G., Förster W., Brettske I., Gerber S., Ginhart A. W., Gross O., Grumann S., Hermann S., Jost R., König A., Liss T., Lussmann R., May M., Nonhoff B., Reichel B., Strehlow R., Stamatakis A., Stuckmann N., Vilbig A., Lenke ., Ludwig T., Bode A., and Schleifer K. H. (2004) ARB: a software environment for sequence data. *Nucleic Acid Research* 32: 1363-1371.

MacGregor B., Moser D.P., Alm E. W., Nealson K. H., and Stahl D. A. (1997) Crenarchaeota in Lake Michigan sediment. *Applied and Environmental Microbiology* 63: 1178-1181.

Martens C. S. (1990) Generation of short chain organic acid anions in hydrothermally altered sediments of the Guaymas Basin, Gulf of California. *Applied Geochemistry* 5:71-76.

Martens, C. S., Albert, D. B., and Alperin, M. J. (1999) Stable isotope tracing of anaerobic methane oxidation in the gassy sediments of Eckernförde Bay, German Baltic Sea. *American Journal of Science* 299: 589–610.

McKay, L. J., MacGregor B. J., Biddle J. F., Mendlovitz H. P., Hoer D., Lipp J. S., Lloyd K. G., and Teske A. P. (2012) Spatial heterogeneity and underlying geochemistry of phylogenetically diverse orange and white *Beggiatoa* mats in Guaymas Basin hydrothermal sediments. *Deep-Sea Research I* 67: 21-31.

McIlroy S., Porter K., Seviour R. J. and Tillett D. (2008) Simple and safe method for simultaneous isolation of microbial RNA and DNA from problematic populations. *Applied and Environmental Microbiology* 74(21): 6806-6807.

Meyer, S., Wegener G., Lloyd K.G., Teske A., Boetius A., and Ramette A. (2013) Microbial habitat connectivity across spatial scales and hydrothermal temperature gradients at Guaymas Basin. *Frontiers in Microbiology* 4: 207

Mills, H. J., Martinez, R. J., Story, S., and Sobecky, P. A. (2004) Identification of members of the metabolically active microbial populations associated with *Beggiatoa* species mat communities from Gulf of Mexico cold-seep sediments. *Applied and Environmental Microbiology* 70: 5447-5458.

Nelson D.C., Wirsen C.O., and Jannasch H.W. (1989) Characterization of large, autotrophic *Beggiatoa* spp. abundant at hydrothermal vents of the Guaymas Basin. *Applied and Environmental Microbiology* 55: 2909-2917.

Orphan V. J., House C. H., Hinrichs K.-U., McKeegan K. D., and DeLong E. F. (2002) Multiple archaeal groups mediate methane oxidation in anoxic cold seep sediments. *Proceedings of the National Academy of Science of the United States of America* 99: 7663-7668.

Pearson A., Seewald J. S., and Eglinton T. I. (2005) Bacterial incorporation of relict carbon in the hydrothermal environment of Guaymas Basin. *Geochimica et Coscochimica Acta* 69: 5477-5486.

Peter J. M. and Shanks W. C. III (1992). Sulfur, carbon, and oxygen isotope variations in submarine hydrothermal deposits of Guaymas Basin, Gulf of California. *Geochimica et Cosmochimica Acta* 56: 2025-2040.

Pruesse E., Quast C., Knittel K., Fuchs B. M., Ludwig W., Peplies J., and Glöckner F. O. (2007). SILVA: a comprehensive online resource for quality checked and aligned ribosomal RNA sequence data compatible with ARB. *Nucleic Acids Research* 35: 7188-7196

Roesch L. F. W., Fulthorpe R. R., Riva A., Casella G., Hadwin A. K., Kent A. D., Daroub S. H., Camargo F. A., Farmerie W. G., and Triplett E. W. (2007) Pyrosequencing enumerates and contrasts soil microbial diversity. *The ISME Journal* 1:283-290.

Saitou N. and Nei M. (1987) The neighbor-joining method: A new method for reconstructing phylogenetic trees. *Molecular Biology and Evolution* 4(4): 406-425.

Schreiber L., Holler T., Knittel K., Meyerdierks A., and Amann R. (2010) Identification of the dominant sulfate-reducing bacterial partner of the anaerobic methanotrophs of the ANME-2 clade. *Environmental Microbiology* 12: 2327–2340.

Shannon C. E. and Weaver W. (1963). *The mathematical theory of communications*. University of Ilinois press. Urbana, p. 117. ISBN: 0-252-72548-4.

Stahl D. A., Flesher B., Mansfield H. R., and Montgomery L. (1988) Use of phylogenetically based hybridization probes for studies of ruminal microbial ecology. *Applied and Environmental Microbiology* 54(5): 1079-1084.

Sørensen K. B. and Teske A. (2006) Stratified communities of active archaea in deep marine subsurface sediments. *Applied and Environmental Microbiology* 72: 4596-4603.

Takai K. and Horikoshi K. (1999) Genetic diversity of archaea in deep-sea hydrothermal vent environments. *Genetics* 152: 1285-1297.

Teske, A., Hinrichs K.-U., Edgcomb V., de Vera Gomez A., Kysela D., Sylva S. P., Sogin M. L., and Jannasch H. W. (2002) Microbial diversity in hydrothermal sediments in the Guaymas Basin: Evidence for anaerobic methanotrophic communities. *Applied and Environmental Microbiology* 68:1994-2007

Teske A. and Sørensen K.B. (2008) Uncultured archaea in deep marine subsurface sediments: have we caught them all? *The ISME Journal* 2: 3-18.

Tor J.M., Kashefi K., and Lovley D. R. (2001) Acetate oxidation coupled to Fe (III) reduction in hyperthermophilic microorganisms. *Applied and Environmental Microbiology* 67(3): 1363-1365.

Vetriani C., Jannasch H. W., MacGregor B. J., Stahl D. A., and Reysenbach A. L. (1999) Population structure and phylogenetic characterization of marine benthic archaea in deep-sea sediments. *Applied and Environmental Microbiology* 65: 4375 – 4384

Von Damm K. L. (1990) Seafloor hydrothermal activity: black smoker chemistry and chimneys. *Annual Reviews of Earth and Planetary Science* 18: 173-204.

Von Damm K. L., Edmonds J. M., Measures C. I., and Grant B. (1985) Chemistry of submarine hydrothermal solutions at Guaymas Basin, Gulf of California. *Geochimica et Cosmochimica Acta* 49: 2221-2237.

Welhan J.A. and Lupton J. E. (1987) Light hydrocarbon gases in Guaymas Basin hydrothermal fluids; thermogenic versus abiogenic origin. *American Association of Petroleum Geologists Bulletin* 71: 215-223.

Whiticar M. J. (1999) Carbon and hydrogen isotope systematics of bacterial formation and oxidation of methane. *Chemical Geology* 161: 291-314.

Wiener N. (1948) *Cybernetics: or Control and Communication in the Animal and Machine*. John Wiley and Sons, New York.